

Discovery of 7-Methyl-5-(1-([3-(trifluoromethyl)phenyl]acetyl)-2,3-dihydro-1*H*-indol-5-yl)-7*H*-pyrrolo[2,3-*d*]pyrimidin-4-amine (GSK2606414), a Potent and Selective First-in-Class Inhibitor of Protein Kinase R (PKR)-like Endoplasmic Reticulum Kinase (PERK)

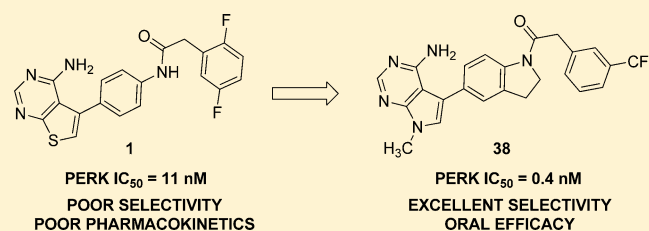
Jeffrey M. Axten,^{*,†} Jesús R. Medina,[†] Yanhong Feng,[†] Arthur Shu,[†] Stuart P. Romeril,[†] Seth W. Grant,[†] William Hoi Hong Li,[†] Dirk A. Heerding,[†] Elisabeth Minthorn,[†] Thomas Mencken,[†] Charity Atkins,[†] Qi Liu,[†] Sridhar Rabindran,[†] Rakesh Kumar,[†] Xuan Hong,^{||} Aaron Goetz,[‡] Thomas Stanley,[§] J. David Taylor,[§] Scott D. Sigethy,[§] Ginger H. Tomberlin,[§] Annie M. Hassell,^{||} Kirsten M. Kahler,^{||} Lisa M. Shewchuk,^{||} and Robert T. Gampe^{||}

[†]Oncology Research, Protein Dynamics DPU, GlaxoSmithKline Research and Development, Collegeville, Pennsylvania 19426, United States

[‡]Screening and Compound Profiling, [§]Biological Reagents and Assay Development, and ^{||}Computational and Structural Chemistry, GlaxoSmithKline Research and Development, Research Triangle Park, North Carolina 27713, United States

Supporting Information

ABSTRACT: Protein kinase R (PKR)-like endoplasmic reticulum kinase (PERK) is activated in response to a variety of endoplasmic reticulum stresses implicated in numerous disease states. Evidence that PERK is implicated in tumorigenesis and cancer cell survival stimulated our search for small molecule inhibitors. Through screening and lead optimization using the human PERK crystal structure, we discovered compound 38 (GSK2606414), an orally available, potent, and selective PERK inhibitor. Compound 38 inhibits PERK activation in cells and inhibits the growth of a human tumor xenograft in mice.



INTRODUCTION

Endoplasmic reticulum (ER) stress resulting from accumulation of unfolded proteins is emerging as an important factor in human diseases such as neurodegeneration, heart disease, diabetes, and cancer.¹ To cope with ER stress, cells activate an evolutionarily conserved mechanism termed the unfolded protein response (UPR), which coordinates an adaptive cellular signaling cascade to alleviate the impact of the stress and enhance cell survival.^{2–4} Under prolonged stress and in environments in which the UPR cannot mitigate the enduring strain, additional pathways may be activated to induce apoptosis or autophagy.⁵ Impairment of the ER capability to properly fold and process proteins can occur under conditions of hypoxia and nutrient deprivation, situations that are commonly found in tumors. Human tumors, including those derived from cervical carcinomas, glioblastomas, lung cancers, and breast cancers, show elevated levels of UPR-related proteins when compared to normal tissues.^{6–9} This, together with evidence signifying a role of the UPR in tumorigenesis, survival, and proliferation of cancer cells, supports the UPR as an attractive pathway for cancer drug discovery.^{2,10}

Protein kinase R (PKR)-like ER kinase (PERK) is one of three primary effectors of the UPR, which has a demonstrated role in tumor growth and angiogenesis.^{11–15} PERK is a type I

ER membrane protein containing a stress-sensing domain facing the ER lumen, a transmembrane segment, and a cytosolic kinase domain.^{16–18} Increase in unfolded proteins in the ER causes release of ER chaperones from the stress-sensing domain of PERK, which results in its activation via oligomerization and autophosphorylation at multiple serine, threonine, and tyrosine residues.^{19–21} Upon activation, PERK phosphorylates eukaryotic initiation factor 2 α (eIF2 α) at serine 51, rendering it an inhibitor of the ribosome translation initiation complex, consequently reducing overall protein synthesis.²² The reduction in translation reduces the ER burden, providing time for the cell to process or degrade the accumulated unfolded proteins to restore ER homeostasis. Although global protein synthesis is decreased, there is specific increased translation of certain mRNAs, such as ATF4, which modulate cellular survival pathways and enhance UPR function. Interfering with PERK function in cancer cells may limit their ability to thrive under hypoxia or nutrient deprived conditions and lead to apoptosis or tumor growth inhibition. Although an attractive potential target for cancer intervention, currently there are no known inhibitors of PERK to probe the role of its

Received: May 21, 2012

Published: July 24, 2012

catalytic function in tumor growth. Herein we describe our discovery of potent and selective PERK inhibitors, which demonstrate the ability to inhibit PERK activity in cells and display growth inhibition of human tumor xenografts in mice.

We identified potent inhibitors of PERK by screening our proprietary collection of kinase inhibitors for activity in a PERK mediated eIF2 α phosphorylation assay. It was anticipated that this strategy would not only quickly deliver lead molecules for medicinal chemistry but also provide added value from existing kinase selectivity data that could influence hit prioritization. Of several classes of inhibitors identified, the thienopyrimidine **1** (Figure 1) was attractive based on its favorable molecular

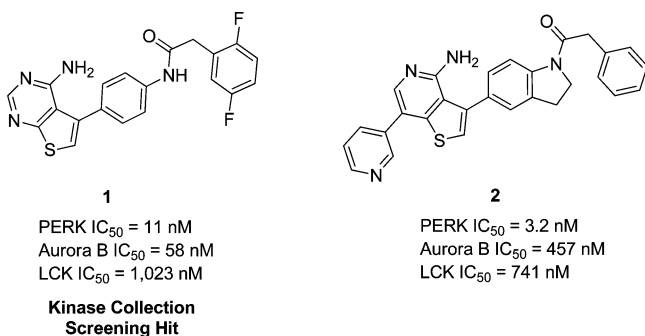


Figure 1. Structures and kinase data for hits identified in a PERK screen.

weight and lipophilicity (MW = 396.4, ClogP = 3.66), potency (PERK IC₅₀ = 11 nM), and selectivity evident in a limited set of kinase inhibition data. For example, of 14 kinases with assay data available, only Aurora B (IC₅₀ = 58 nM) and LCK (IC₅₀ = 1023 nM) showed inhibition within 100-fold the concentration needed for similar PERK inhibition. Follow-up screening of related analogues within the corporate compound collection led to our discovery of compound **2**, which contained an indoline as the core structure. The indoline **2** had increased potency (PERK IC₅₀ = 3.2 nM) and offered higher kinase selectivity against Aurora B and LCK relative to the anilide **1** (e.g., Aurora B IC₅₀ of 457 nM vs 58 nM for **1**). On the basis of this profile, we initiated a lead optimization campaign based on indoline **2**.

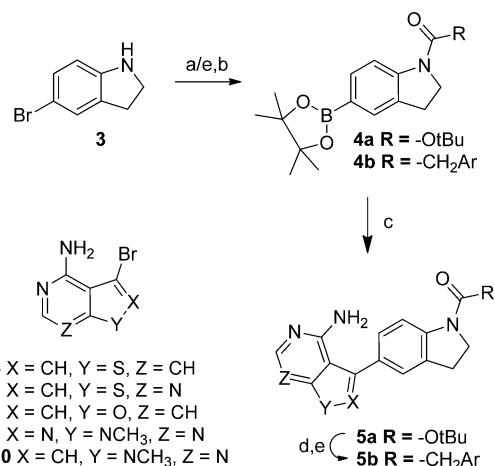
CHEMISTRY

A convergent synthetic route was devised to allow for flexible variation of three components of the molecules: the hinge binder heterocyclic system, the indoline core, and the arylacetamide. We synthesized indoline boronate derivative **4a** in two steps from commercially available 5-bromoindoline **3** (Scheme 1). This building block allowed for diverse functionalization and rapid synthesis of analogues. Suzuki–Miyaura coupling of **4a** with heteroaryl bromides **6–10** gave intermediate **5a**. Boc group removal under acidic conditions liberated the indoline, which was then coupled with arylacetic acids to give the target compounds represented by **5b**. Alternatively, the boronate **4b** was synthesized first and subjected to Suzuki–Miyaura coupling to afford **5b**.

The heteroaryl bromides **6**, **8**, and **9** are commercially available or have been previously described. Compounds **7** and **10** were prepared as shown in Scheme 2 from commercially available intermediates **11** and **12**.

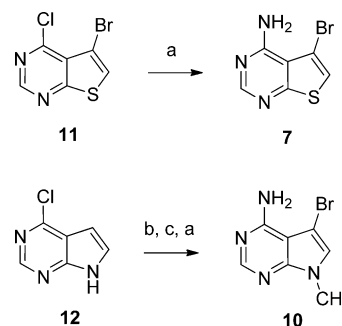
We were unable to efficiently prepare the 3-bromofuranopyrimidine hinge binder for use in the Suzuki–Miyaura coupling. Therefore, for this analogue we annulated the pyrimidine ring

Scheme 1^a



^a(a) Boc₂O, DMAP, CH₃CN, 71%; (b) bis(pinacolato)diboron, KOAc, PdCl₂(dppf); (c) heteroaryl bromides **6–10**, Suzuki–Miyaura conditions; (d) HCl, ethanol; (e) arylacetic acid, EDC or HATU, DIPEA, DMF.

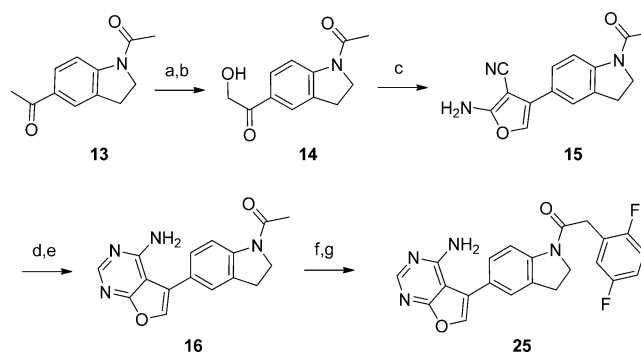
Scheme 2^a



^a(a) conc NH₄OH, 80–86%; (b) NaH, CH₃I, DMF, 74%; (c) NBS, CH₂Cl₂, 95%.

onto a suitable substituted furan (Scheme 3). Hydroxylation of 1,5-diacetylindoline **13** was performed by a halogenation, nucleophilic displacement, and hydrolysis sequence to give **14**. Reaction of **14** with malononitrile formed the substituted furan **15**, which was then converted to the furanopyrimidine **16**.

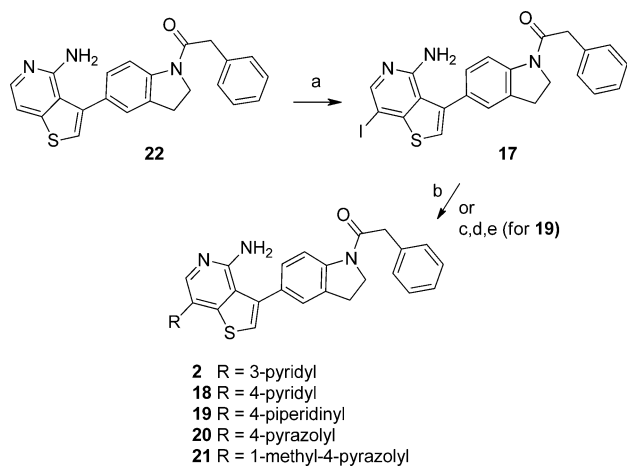
Scheme 3^a



^a(a) pyridine-HBr₃, THF, 93%; (b) NaOAc, then NaOH, 80%; (c) malononitrile, Et₂NH, DMF, 80%; (d) (EtO)₂CHOAc, 1,4-dioxane, 76%; (e) NH₃, MeOH, 90%; (f) KOH, EtOH, DMSO, 47%; (g) HATU, (2,5-difluorophenyl)acetic acid, DIPEA, DMF, 32%.

Hydrolysis of the acetamide gave the indoline which was coupled with (2,5-difluorophenyl)acetic acid to provide compound **25**.

Direct iodination was used as a means to introduce a variety of substituents at the 7-position of the bicycloheteroaryl ring (Scheme 4). Transition metal mediated coupling and deprotection (if necessary) afforded analogues **2** and **19–21**.

Scheme 4^a

^a(a) NIS, DMF, 93%; (b) *R*-pinacol boronate, PdCl₂(dppf)–CH₂Cl₂ adduct, NaHCO₃, dioxane–H₂O, 53–85%; (c) 3,6-dihydro-2*H*-pyridine-1-*N*-Boc-4-boronic acid pinacol ester, PdCl₂(dppf)–CH₂Cl₂ adduct, NaHCO₃, dioxane–H₂O, 85%; (d) 10% Pd/C, THF, EtOH, 40 bar of H₂, 41%; (e) TFA, DCM, 47%.

RESULTS AND DISCUSSION

Lead Optimization and SAR. At the initiation of our research, there was no structural data available for PERK. On the basis of kinase inhibitor structural motifs, we presumed that the thienopyridine of **2** acted as a kinase β -strand hinge binder and that the indoline core served as a scaffold to orient the arylacetamide toward a back pocket of the PERK ATP binding site, enabling productive interactions with the protein. We began our optimization of **2** by interrogating the importance of the pyridine substituent, which we believed was oriented toward solvent based on this model. A small increase in potency was realized with 4-pyridyl substitution (**18**, PERK IC₅₀ = 1.2 nM, Table 1) or with pyrazole replacements (**20** and **21**, PERK IC₅₀ of 0.9 and 1.3 nM). Interestingly, we could substitute this position with an aliphatic cyclic amine with little effect on PERK potency. For example, the piperidine analogue **19** maintained PERK activity (IC₅₀ = 1.9 nM) and offered a path to increasing compound solubility and polarity. Although removing the pyridyl group resulted in ~4-fold loss of potency, we were encouraged by the increased ligand efficiency of **22** (PERK IC₅₀ = 11.7 nM, LE = 0.39). Reintroducing the 2,5-difluoro substitution found in the screening hit gave compound **23** which was a slightly more active PERK inhibitor than **2** with increased ligand efficiency (LE of 0.39 vs 0.34), an attractive attribute to consider in the optimization of oral drugs.²⁴ In addition, we also observed some improvement in kinase selectivity without the aromatic group at R₂ (data not shown). This is consistent with the presumed hinge binding motif in which the aryl group fills the lipophilic plug conserved among most kinases.²⁵ By elimination of this interaction, the

Table 1. PERK Inhibitory Data for Thieno[3,2-*c*]pyridin-4-amine Analogues

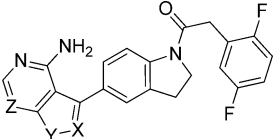
Entry	R ₁	R ₂	PERK IC ₅₀ (nM) ^a	LE ^b
2			3.2 ± 1.9	0.34
18			1.2 ± 0.52	0.36
19			1.9 ± ND ^c	0.35
20			0.9 ± 0.03	0.38
21			1.3 ± 0.22	0.36
22		H	11.7 ± ND	0.39
23		H	2.5 ± 0.67	0.39

^aInhibitory activity as measured by cytoplasmic PERK domain phosphorylation of EIF2 α . Average values are reported with standard deviation (see Experimental Section for details). ^bLE = ligand efficiency, defined as $\Delta G/N_{\text{non-hydrogen atoms}}$, where $\Delta G \approx -RT \ln(\text{IC}_{50})$. ^cND = not determined (data reported from a single experiment).

specificity for PERK improved because of reliance on specific interactions deep in the PERK binding site (see discussion below).

The thieno[3,2-*c*]pyridin-4-amine analogues were quite lipophilic and generally displayed potent P450 inhibition, high metabolic turnover, and poor pharmacokinetic parameters (data not shown). Therefore, we set out to increase the overall polarity of the molecules through variation of the hinge binding heteroaryl group (Table 2). Exchanging a nitrogen for carbon in **23** gave the thieno[2,3-*d*]pyrimidin-4-amine **24**, lowering the ClogP by 0.6 units to 4.1 and improving PERK activity 4-fold. Further reductions in ClogP were accomplished by varying the type and placement of heteroatoms. The furo[2,3-*d*]pyrimidin-4-amine **25**, furo[3,2-*c*]pyridin-4-amine **26**, and pyrazolo[3,4-*d*]pyrimidin-4-amine **27** analogues were less active than the thieno derivatives **23** and **24**. However, the pyrrolo[2,3-*d*]pyrimidin-4-amine **28** afforded a 6-fold increase in potency relative to **23**, at the same time lowering the ClogP by 1.2 units. The reduction in lipophilicity of **25**, **27**, and **28** corresponded with improved rat blood clearance within a desirable range below hepatic blood flow. Since all of these hinge binder analogues theoretically meet size and shape requirements for

Table 2. PERK Inhibition and Pharmacokinetic Data for Hinge Binder Analogues



compd	X	Y	Z	PERK IC ₅₀ (nM) ^a	ClogP ^b	rat Cl _b (mL min ⁻¹ kg ⁻¹) ^c
23	CH	S	CH	2.5 ± 0.67	4.7	ND ^d
24	CH	S	N	0.6 ± ND	4.1	42.7
25	CH	O	N	7.4 ± 1.12	3.4	26.3
26	CH	O	CH	8.1 ± ND	4.0	89.7
27	N	N-CH ₃	N	5.4 ± 1.92	2.9	31.0
28	CH	N-CH ₃	N	0.4 ± 0.10	3.5	21.2

^aInhibitory activity as measured by cytoplasmic PERK domain phosphorylation of EIF2 α . Average values are reported with standard deviation (see Experimental Section for details). ^bCalculated using BioByte cLogP (the calculated logarithm of the 1-octanol–water partition coefficient of the nonionized molecule, see www.biobyte.com). ^cAverage in vivo blood clearance determined after iv infusion in SD rats ($n = 2$). ^dNot determined.

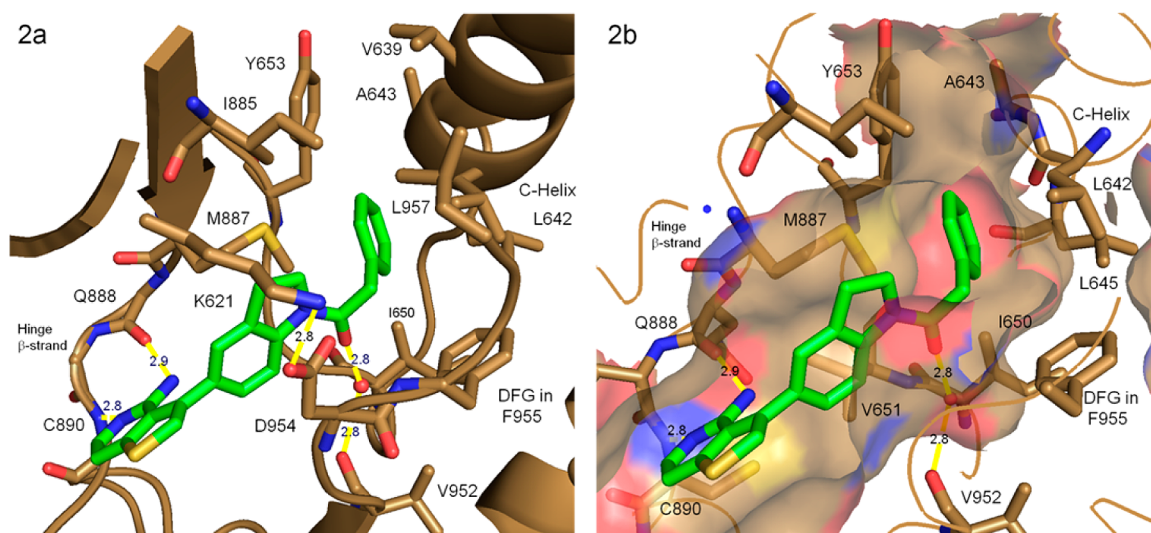


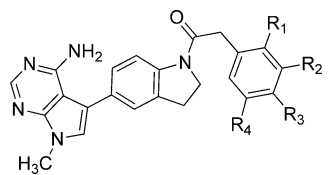
Figure 2. Crystal structure of compound **22** bound to the PERK kinase domain: (a) close-up view of **22** (green sticks) in the PERK active site (brown cartoon and sticks); (b) close-up view of **22** bound to the PERK active site with surface rendering. The indoline fills a narrow channel between M887 and D954 of the inward facing DFG motif. The aryl ring occupies a portion of a large lipophilic pocket. Protein residues and structural motifs are labeled. Atomic interactions are indicated with yellow lines and distances reported in angstrom.

PERK binding, the SAR reveals that additional forces such as electrostatics are integral to optimal PERK inhibition.

During our optimization, we determined the crystal structure of **22** bound to the human PERK kinase domain.²³ The PERK structure is consistent with the global canonical fold of kinase domains where the N- and C-terminal lobes are connected by the intervening hinge β -strand that forms part of the ATP or inhibitor binding cleft (Figure 2). Adjacent to the inhibitor binding site, the catalytic lysine, K621, forms a salt bridge with D954 of the inward facing DFG motif (Figure 2a). Respectively, residues Q888 and C890 of the hinge β -strand accept and donate hydrogen bonds to the inhibitor's thieno-[3,2-*c*]pyridin-4-amine moiety. The indoline ring system fills a narrow channel between the lipophilic gatekeeper, M887, and the inward facing DFG motif, orienting the carboxamide for favorable interactions. The carboxamide carbonyl participates in a water mediated hydrogen bond to the backbone carbonyl of V952 and the NH of V651 (Figure 2b). The acetamide aryl ring is contained by a large lipophilic pocket formed in part by the side chains from the M887 gatekeeper, the α -helix L642, and F955 of the DFG motif (Figure 2b) as well as L645, I650,

Y653, and I885. From the structure it was apparent that unfilled hydrophobic space was available above the aryl ring meta-position.

Utilizing the PERK crystal structure and analysis of **22** bound as a design aid, we prepared numerous substituted arylacetamides to probe the SAR of this moiety. Table 3 provides data for selected analogues in our study. In comparison to the 2,5-difluorophenyl analogue **28** (PERK IC₅₀ = 0.4 nM), the ortho- and meta-monofluorinated compounds **29** and **30** showed little difference in potency (PERK IC₅₀ of 0.7 and 0.2 nM, respectively) but were 2- to 5-fold more active than the para-fluoro analogue **31** (PERK IC₅₀ = 1.5 nM). Likewise, the activity was maintained with ortho- and meta-chlorine substitution in **35** and **36**, with a slight preference for the meta-chloroacetamide **36** (PERK IC₅₀ of 0.2 nM vs 0.9 nM for **35**). The ortho- and meta-CH₃ analogues **32** and **33** were equipotent (PERK IC₅₀ = 0.2 nM); however, the para-CH₃ analogue **34** (PERK IC₅₀ = 17.4 nM) lost a significant amount of activity, likely because of steric contacts with the protein. These results are consistent with the structural data, which indicates that the small, tight space between the

Table 3. Summary of SAR for Arylacetamides of the Pyrrolo[2,3-*d*]pyrimidin-4-amine Series


compd	R ₁	R ₂	R ₃	R ₄	PERK IC ₅₀ (nM) ^a	ClogP ^b	rat Cl _b (mL min ⁻¹ kg ⁻¹) ^c
28	F	H	H	F	0.4 ± 0.10	3.5	21.2
29	F	H	H	H	0.7 ± 0.13	3.4	46.4 ^d
30	H	F	H	H	0.2 ± ND ^e	3.4	49.6
31	H	H	F	H	1.5 ± 1.19	3.4	16.5 ^d
32	CH ₃	H	H	H	0.2 ± ND ^e	3.7	71.2
33	H	CH ₃	H	H	0.2 ± ND ^e	3.7	110.1
34	H	H	CH ₃	H	17.4 ± ND ^e	3.7	ND ^e
35	Cl	H	H	H	0.9 ± 0.28	3.9	ND ^e
36	H	Cl	H	H	0.2 ± ND ^e	3.9	46.7
37	H	OCH ₃	H	H	0.5 ± 0.12	3.2	ND ^e
38 (GSK2606414)	H	CF ₃	H	H	0.4 ± 0.32	4.11	21.5 ^d
39	H	CF ₃	H	F	0.3 ± 0.32	4.3	17.7 ^d
40	F	F	H	F	0.2 ± 0.01	3.6	8.3

^aInhibitory activity as measured by cytoplasmic PERK domain phosphorylation of EIF2 α . Average values are reported with standard deviation (see Experimental Section for details). ^bCalculated using BioByte cLogP (the calculated logarithm of the 1-octanol–water partition coefficient of the nonionized molecule, see www.biobyte.com). ^cUnless noted, rat clearance data reported were obtained by cassette dosing (up to three compounds) as an iv infusion (2 mg/kg target dose). ^dDiscrete dosing ($n = 2$) as an iv infusion (2 mg/kg target dose). ^eND = not determined.

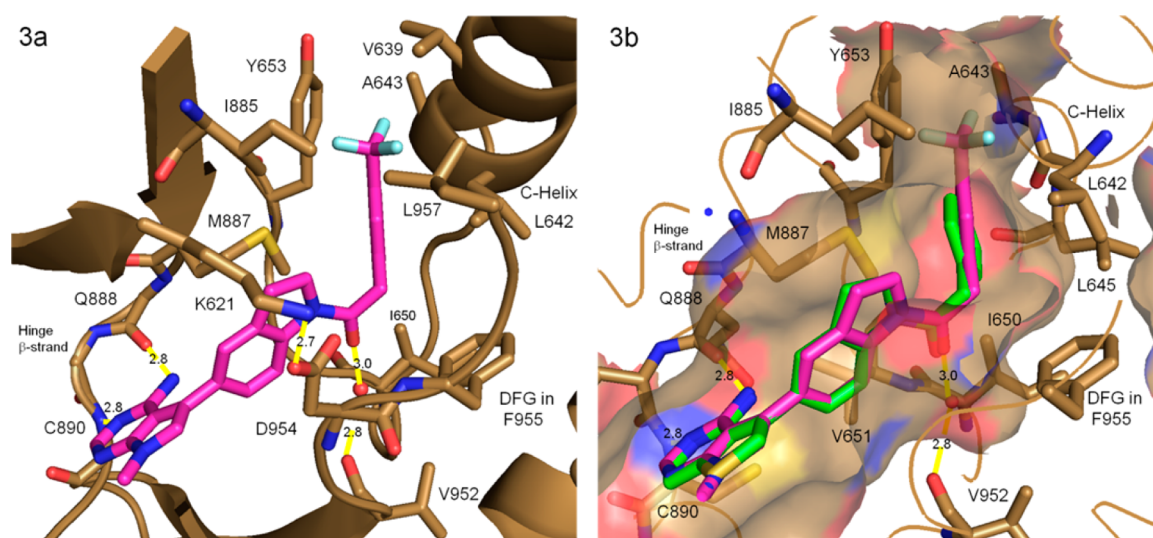


Figure 3. Crystal structure of **38** bound to PERK kinase domain: (a) close-up view of **38** (magenta sticks) in the PERK active site (brown cartoon and sticks); (b) close-up view of **38** superimposed upon the structure of **22** (green sticks) bound to the PERK active site with surface rendering. PERK accommodates a meta-CF₃ substituent that fills the lipophilic space above the aryl ring but does not provide room for para-substitution. Protein residues and structural motifs are labeled. Atomic interactions are indicated with dashed yellow lines with distances reported in angstrom.

Y653 side chain and A643 of the C- α helix is not likely to accommodate a bulky para-substituent on the arylacetamide. Electron donating and withdrawing groups were tolerated, as demonstrated by the activity of the meta-methoxy and meta-trifluoromethyl compounds **37** and **38** (PERK IC₅₀ of 0.5 and 0.4 nM, respectively). An X-ray structure of **38** bound to PERK was solved (Figure 3) and shows similar features and interactions as those described for the thieno[3,2-*c*]pyridin-4-amine **22**. Furthermore, the structure reveals that the trifluoromethyl meta-substituent occupies the lipophilic volume bounded by the side chains of C- α helix residues, L642, A643 and also Y653, I885, and the aryl ring lies between the side chains of L642 and the M887 gatekeeper.

During the course of our optimization, we evaluated the in vivo rat blood clearance of analogues to gain insight into the influence of the arylacetamide substitution pattern on metabolism. An increase in clearance was observed in the potent compounds **32** and **33**, consistent with additional oxidative metabolism of the exposed methyl groups (Table 3). A significant decrease in rat blood clearance was measured for the para-fluorophenyl analogue **31** (Cl_b = 16.5 mL min⁻¹ kg⁻¹), in contrast to the ortho- and meta- substituted analogues **29** and **30** which displayed moderate to high clearance (Cl_b of 46.4 and 49.6 mL min⁻¹ kg⁻¹, respectively). These data implied that the phenyl para-position was a metabolic liability and likely a location of aromatic oxidation. Blocking the suspected

oxidation site was not an option because para-substitution was detrimental to PERK inhibitory activity. Therefore, we pursued a strategy of reducing the electron density of the aryl ring to decrease susceptibility to aromatic oxidation. The 3-trifluoromethylphenylacetamide **38** and 5-fluoro-3-trifluoromethylphenylacetamide **39** maintained moderate rat clearance in the range of 17–19 mL min⁻¹ kg⁻¹. The 2,3,5-trifluorophenylacetamide **40** exhibited a dramatic decrease in clearance (Cl_b = 8.3 mL min⁻¹ kg⁻¹), confirming that we could indeed influence the pharmacokinetic properties by arylacetamide modification while maintaining potent PERK inhibitory activity.

Characterization of Cell Activity. Compounds in this study with potent PERK activity were routinely screened for the ability to affect PERK function in cells. Analogues were evaluated for their ability to prevent PERK activation upon treatment of A549 cells with thapsigargin, a chemical inducer of the UPR. Activity was assessed in a gel-based assay measuring inhibition of thapsigargin induced autophosphorylation of PERK in the presence of 0.03, 0.1, and 0.3 μM inhibitor. Western blots for compounds **2**, **21**, and **38** are shown in Figure 4 as representative examples. Compound **38** completely

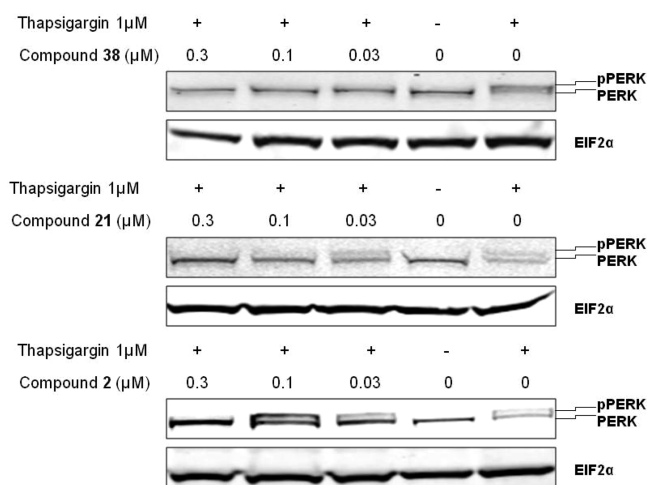


Figure 4. Representative Western blots for compounds **2**, **21**, and **38** showing a range of PERK inhibition in A549 cells. Cells were incubated with PERK inhibitor and then stimulated with thapsigargin. After 2 h, the cells were lysed and analyzed by Western blot for inhibition of PERK autophosphorylation. See Experimental Section for details.

inhibits PERK phosphorylation at the lowest concentration in this assay. Compounds **21** and **2** require higher concentrations to fully inhibit PERK phosphorylation, and these data were used to estimate IC₅₀ values for PERK autophosphorylation. Table 4 contains estimated IC₅₀ data for selected compounds with potent PERK activity and low to moderate rat blood clearance. All compounds inhibit activation of PERK at levels consistent with the in vitro biochemical data.

Kinase Selectivity Profiling. Since PERK is a member of the eIF2α-kinase (EIF2AK) family, selected PERK inhibitors were assayed against HRI and PKR (available kinases within the EIF2AK family) to assess selectivity (Table 5). All compounds tested were selective and displayed at least 100-fold selectivity over the other EIF2AKs assayed. The high specificity for PERK within the EIF2AK family is impressive and was not predicted based on the high similarity of the active sites. We hypothesize that the high selectivity arises from the ability of the inhibitors

Table 4. Compounds Inhibit PERK Autophosphorylation in A459 Cells

compd	phospho-PERK IC ₅₀ (μM) ^a
2	0.1–0.3
21	0.03–0.1
22	>0.3
28	0.03–0.1
31	0.1–0.3
36	<0.03
38	<0.03
40	0.03–0.1

^aIC₅₀ estimated from a Western blot three-point dose response. See Experimental Section for details.

Table 5. EIF2AK Selectivity Data for PERK Inhibitors

compd	EIF2AK3 (PERK) IC ₅₀ (nM) ^a	EIF2AK1 (HRI) IC ₅₀ (nM) ^b	EIF2AK2 (PKR) IC ₅₀ (nM) ^b
38	0.4	420	696
21	1.3	1863	978
36	0.2	214	291
2	3.2	12080	>10000
22	11.7	17020	>10000

^aInhibitory activity as measured by cytoplasmic PERK domain phosphorylation of EIF2α. Values reported are the average of at least two experiments (see Experimental Section for details). ^bData from a single 10-point dose response performed by Reaction Biology Corp. (<http://www.reactionbiology.com>).

to trap an inactive PERK conformation. This is supported by (1) the recently published structure²⁶ of active mouse PERK revealing an active site pocket that could not accommodate our inhibitors, although they are similarly active against the mouse protein (data not shown), and (2) our inhibitors also exhibit time-dependent PERK inhibition and extremely slow off-rates, consistent with binding to an inactive kinase conformation.²⁷

On the basis of the EIF2AK selectivity profile, cellular potency, and rat blood clearance, compound **38** was screened against a panel of 294 kinases to further evaluate selectivity. Overall, good selectivity was observed, with only 20 protein kinases inhibited >85% by **38** at 10 μM.²⁸ We subsequently determined IC₅₀ values for each of those kinases (Table 6). The most sensitive kinase (c-kit, IC₅₀ = 154 nM) is 385-fold less sensitive than PERK (IC₅₀ = 0.4 nM), confirming the outstanding selectivity of compound **38**.

Pharmacokinetics.²⁹ Pharmacokinetic profiling was performed in mouse, rat, and dog for compound **38** (Table 7). Compound **38** was well absorbed providing good exposure, high oral availability, and low to moderate blood clearance in mouse, rat, and dog. Estimated volume of distribution at steady state was moderate to high in the three species.

Efficacy in Human Tumor Xenograft Experiments.²⁹ Compound **38** was advanced to an efficacy study to gauge effects of a PERK inhibitor on the growth of tumors in mice. Compound **38** was administered orally twice a day for 21 days to mice bearing subcutaneous pancreatic human BxPC3 tumors. Tumor growth was measured over the course of the study and is presented in Figure 5. When compared to vehicle control, compound **38** inhibited tumor growth in a dose-dependent manner, demonstrating 20% and 59% tumor growth inhibition at doses of 50 and 150 mg/kg b.i.d. × 21 days, respectively. Furthermore, the compound was well tolerated with no overt signs of toxicity or changes in body weight.

Table 6. Kinase Inhibitory Data for Compound 38^a

kinase	IC ₅₀ (nM)	kinase	IC ₅₀ (nM)
c-kit	154	RET	1215
Aurora B	407 ^b	LCK	1250
BRK	412	NEK4	1402
MLK2/MAP3K10	452	KHS/MAP4K5	1569
c-MER	474	MLK1/MAP3K9	1578
DDR2	524	TRKA	1756
MLCK2/MYLK2	701	AXL	2705
IKKe/IKBKE	1064	TRKB	2962
TRKC	1115	YES/YES1	3195
MLK3/MAP3K11	1140	WNK2	3892

^aUnless noted, data obtained from a single 10-point dose response performed by Reaction Biology Corp. (<http://www.reactionbiology.com>). ^bAverage of at least two experiments from an internal kinase assay.

CONCLUSIONS

We have discovered a series of first-in-class PERK inhibitors. Optimization of biochemical activity and pharmacokinetics of the indoline series was achieved by individual improvements to each structural component of the inhibitor. The β -strand hinge binder, indoline ring, and arylacetamide groups of the inhibitors each participate in favorable interactions with PERK as determined by crystallographic studies and SAR. Throughout our investigation, the electronic nature of the aromatic ring systems was utilized as a means to positively influence potency and pharmacokinetics. We established that these PERK inhibitors are functionally active in cells and inhibit PERK signal transduction. Moreover, compound 38 was advanced to a human xenograft efficacy study in mice and demonstrated that small molecule inhibition of PERK can inhibit tumor growth in vivo, consistent with the slow growth of tumors derived from transformed PERK^{-/-} mouse embryonic fibroblasts.^{6,30} Further optimization offering improvements to the physical properties and pharmacokinetics of 38 will be the subject of a future communication.

Because of its potency and superb target selectivity, the PERK inhibitor 38 (GSK2606414) will serve as an excellent tool compound to dissect the UPR and define the role of PERK catalytic activity in a variety of biological systems spanning multiple therapeutic areas.¹

EXPERIMENTAL SECTION

PKR-like Endoplasmic Reticulum Kinase (PERK) Assay (HTRF Format). GST-PERK (no. 536-1116) cytoplasmic domain was

Table 7. Pharmacokinetic Parameters of Compound 38^a

	mouse ^c	rat ^d	dog ^e
iv dose (mg/kg)	1.7	2.1	2.7
AUC _{0-t} (ng·h/mL)	839.1 (732.9–945.3)	1602.1 (1439.6–1764.5)	3155.3 (2653.0–4127.8)
CL _b (mL min ⁻¹ kg ⁻¹)	31.8 (25.8–37.8)	21.5 (19.3–23.6)	12.5 (7.8–14.9)
Vd _{ss} (L/kg)	5.1 (4.2–5.9)	3.8 (3.4–4.2)	8.2 (8.0–8.5)
T _{1/2} (h)	2.5 (2.0–2.9)	2.5 (2.0–2.9)	10.6 (8.0–13.8)
oral dose (mg/kg)	18.3 (suspension)	4.2	4.1
AUC _{0-t} (ng·h/mL)	6017.1 (4186.6–7847.6)	6575.8 (4825.9–8325.7)	3848.5 (2088.9–7094.8)
oral F (%)	62 ^b	~100	72 (52–100)

^aData are reported as the mean, with ranges provided in parentheses. ^bBioavailability (F) was estimated using mean AUC_{0-t} values because of the noncrossover study design. ^cMouse iv: 1% DMSO and 8% Captisol in saline, pH 4. Oral suspension: 0.5% HMPC/0.1% Tween 80 (aq), pH 4. ^dRat iv: 1% DMSO and 8% Captisol in saline, pH 4 (*n* = 2). Oral solution: 1% DMSO and 20% PEG 400 in water, pH 4 (*n* = 2). ^eDog iv: 1% DMSO/20% Captisol in saline, pH 5.69 (*n* = 3). Dog po: 1% DMSO/40% PEG 400 in water, pH 6.11 (homogeneous suspension, *n* = 3).

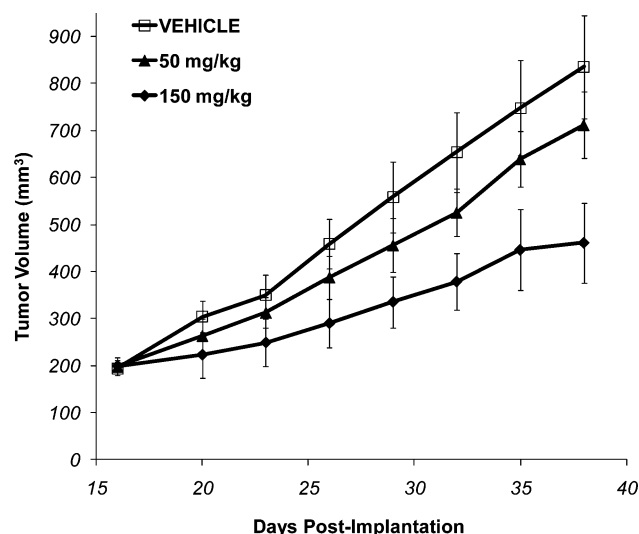


Figure 5. Antitumor activity of 38 in a human pancreatic tumor xenograft model. BxPC3 tumor cells were injected subcutaneously in the flank of female nude mice. Mice with established tumors (~200 mm³) were randomized into treatment groups (*n* = 8 mice/group) and administered 38 orally at 50 and 150 mg/kg b.i.d. for 21 days. Tumor volume measurement and statistical analysis is described in the Experimental Section.

purchased from Invitrogen (catalogue no. PV5106, www.invitrogen.com). 6-His-full-length human eIF2 α was purified from baculovirus expression in Sf9 insect cells. The eIF2 α protein was buffer exchanged by dialysis into PBS, chemically modified by NHS-LC-biotin and then buffer exchanged by dialysis into 50 mM Tris, pH 7.2, 250 mM NaCl, 5 mM DTT. Protein was aliquoted and stored at -80 °C. Quench solution was freshly prepared and when added to the reaction gives final concentrations of 4 nM eIF2 α phospho-ser51-antibody (purchased from Millipore, catalogue no. 07-760, www.millipore.com), 4 nM Eu-1024 labeled anti-rabbit IgG (purchased from Perkin-Elmer, catalogue no. AD0083), 40 nM streptavidin Surelight APC (purchased from Perkin-Elmer, catalogue no. AD0201), and 15 mM EDTA. Reactions were performed in black 384-well polystyrene low volume plates (Grenier, catalogue no. 784076) in a final volume of 10 μ L. The reaction volume contains, in final concentrations, 10 mM HEPES, 5 mM MgCl₂, 5 μ M ATP, 1 mM DTT, 2 mM CHAPS, 40 nM biotinylated 6-His-eIF2 α , and 0.4 nM GST-PERK (no. 536-1116).

Compounds under analysis were dissolved in DMSO to 1.0 mM and serially diluted 1–3 with DMSO through 11 dilutions. An amount of 0.1 μ L of each concentration was transferred to the corresponding well of an assay plate. This creates a final compound concentration range from 0.00017 to 10 μ M.

GST-PERK solution was added to assay plates containing compounds and preincubated for 30 min at room temperature. The reaction was initiated by the addition of ATP and eIF2 α substrate solution. After 1 h of incubation, the quench solution was added. The plates were covered for 2 h at room temperature prior to determination of signal. The resulting signal was quantified on a Viewlux reader (PerkinElmer). The APC signal is normalized to the europium signal by transforming the data through an APC/Eu calculation.

The data for concentration response curves were plotted as % inhibition calculated with the data reduction formula $100 \times [1 - (U_1 - C_2)/(C_1 - C_2)]$ versus concentration of compound where U is the unknown value, C_1 is the average control value obtained for 1% DMSO, and C_2 is the average control value obtained for 0.1 M EDTA. Data were fitted with a curve described by

$$Y = A + [(B - A)/(1 + (10^x/10^c)^D)]$$

where A is the minimum response, B is the maximum response, D is the slope factor, x is the concentration of the compound, and C is the IC_{50} . The results for each compound were recorded as IC_{50} values.

PERK Phosphorylation in A549 Cells. Exponentially growing A549, a human lung adenocarcinoma cell line, was plated at 500 000 cells/well in a six-well dish in RPMI-1640 medium supplemented with 10% fetal bovine serum (FBS) and incubated overnight at 37 °C, 5% CO₂. The following morning, cells were treated with DMSO or compound (3-fold dilutions 0.33, 0.11, 0.37 μ M) and incubated as described above for 1 h. Cells were then stimulated with 1 μ M thapsigargin for an additional hour to induce ER stress. Cells pellets were collected and lysed in cold RIPA buffer [150 mM NaCl, 50 mM Tris-HCl, pH 7.5, 0.25% sodium deoxycholate, 1% NP-40, protease and phosphatase inhibitors (Roche Diagnostics, Indianapolis, IN), and 100 mM sodium orthovanadate (Sigma Aldrich)]. Clarified lysates were resolved by SDS-PAGE and transferred to nitrocellulose membrane using Invitrogen's NuPAGE system. Blots were incubated with primary antibodies to total PERK (R&D Systems) and total eIF-2 α (Cell Signaling Technologies). IRDye700DX-labeled goat anti-mouse IgG and IRDye800-CW donkey anti-goat IgG (LI-COR Biosciences, Lincoln, NE) were used as secondary antibodies. Proteins were detected on the Odyssey infrared imager (LI-COR Biosciences, Lincoln, NE).

Pharmacokinetic Studies. All studies were conducted after review by the Institutional Animal Care and Use Committee at GSK and in accordance with the GSK Policy on the Care, Welfare and Treatment of Laboratory Animals. Pharmacokinetics were studied in male Sprague-Dawley rats, male beagle dogs, and/or male CD-1 mice following single intravenous and/or oral administration. Absolute oral bioavailability was estimated using a crossover study design (n of 2 or 3), unless otherwise indicated. Blood samples were assayed using protein precipitation followed by LC/MS/MS analysis, and the resulting concentration-time data were analyzed by noncompartmental methods (WinNonlin Professional, version 4.1).

BxPC3 Human Pancreatic Xenograft Model. All studies were conducted after review by the Institutional Animal Care and Use Committee at GSK and in accordance with the GSK Policy on the Care, Welfare and Treatment of Laboratory Animals. Exponentially growing BxPC3 tumor cells (10×10^6 cells/mouse) from cell culture were implanted subcutaneously into the right flank of female nude mice (Charles River). Sixteen days after implantation, mice with ~ 200 mm³ tumors were randomized into various treatment groups ($n = 8$ mice/group). Animals were orally treated with vehicle (0.5% hydroxypropylmethylcellulose, 0.1% Tween 80 in water, pH 4.8), compound **38** at 50 or 150 mg/kg, b.i.d. for 21 days. Tumor volume was measured twice weekly with calipers and calculated using the following equation: tumor volume (mm³) = (length \times width)²/2. Results are represented as percent inhibition on completion of dosing, which is $100[1 - (\text{average growth of drug-treated population})/(\text{average growth of vehicle-treated control population})]$. Statistical analysis was performed using a two-tailed t test.

Chemistry. Unless otherwise noted, commercially available materials were used without further purification. Heteroaryl bromides

6,³¹ **8**,³¹ and **9**³² were prepared as previously described. Air or moisture sensitive reactions were carried out under a nitrogen or argon atmosphere. Anhydrous solvents were obtained from Sigma-Aldrich and used as received. Flash chromatography was performed using silica gel under standard techniques or with silica gel cartridges on an Analogix flash chromatography instrument. NMR spectra were recorded on a Bruker 400 MHz spectrometer. Chemical shifts (δ) are quoted in parts per million (ppm) relative to an internal solvent reference. Coupling constants (J) are recorded in hertz. LC-MS analyses were performed on a Sciex or Agilent open access instrument. Analytical HPLC data were recorded with an analytical C18 column, eluting with an acetonitrile/water (+0.1% TFA) gradient over 4 min. Compounds were detected by UV (254, 214, and 333 nm). All final compounds with reported biological data were determined to be >95% pure based on LC-MS, NMR, and analytical HPLC data unless otherwise noted.

1,1-Dimethylethyl 5-(4,4,5,5-Tetramethyl-1,3,2-dioxaborolan-2-yl)-2,3-dihydro-1H-indole-1-carboxylate (4a). To a stirred solution of 5-bromo-2,3-dihydro-1H-indole (30 g, 151 mmol) and DMAP (0.4 g, 3.27 mmol, 0.02 equiv) in 150 mL of CH₃CN at room temperature was added Boc₂O (43 g, 197 mmol, 1.3 equiv) in one portion. The mixture was stirred at room temperature. After 10 min, the mixture gradually became a suspension. After 3 h, the suspension was filtered. The cake was washed with cold CH₃CN (60 mL) and dried under house vacuum for 5 h to give 1,1-dimethylethyl 5-bromo-2,3-dihydro-1H-indole-1-carboxylate (~ 28.5 g prior to drying). The filtrate was concentrated in vacuo, and the residue was partitioned between CH₂Cl₂ (300 mL) and water (250 mL). The organic was dried over Na₂SO₄, filtered, and concentrated in vacuo to give a thick oil (~ 30 g). This material was purified by silica gel chromatography using gradient elution of 1% EtOAc in hexane to 50% EtOAc in hexane. The combined fractions containing product were concentrated, and the solid residue was triturated in cold CH₃CN (25 mL). The resulting paste was filtered, and the cake was washed with cold CH₃CN (5 mL), combined with the above lot, and then dried under vacuum at room temperature for 18 h to give 1,1-dimethylethyl 5-bromo-2,3-dihydro-1H-indole-1-carboxylate (32.14 g, 71%). LC-MS (ES) $m/z = 244, 242$ as prominent fragments [$M - ^t\text{Bu}^+$]. ¹H NMR (400 MHz, DMSO-*d*₆) 1.50 (s, 9 H), 3.06 (t, $J = 8.7$ Hz, 2 H), 3.91 (t, $J = 8.7$ Hz, 2 H), 7.31 (dd, $J = 8.5, 1.9$ Hz, 1 H), 7.38 (s, 1 H), 7.51–7.71 (br s, 1 H).

A mixture of 1,1-dimethylethyl 5-bromo-2,3-dihydro-1H-indole-1-carboxylate (32 g, 107 mmol, 1 equiv), bis(pinacolato)diboron (32.7 g, 129 mmol, 1.2 equiv), PdCl₂(dppf)CH₂Cl₂ adduct (4.38 g, 15.37 mmol, 0.05 equiv), and potassium acetate (26.3 g, 268 mmol, 2.5 equiv) in 350 mL of dioxane in a 1 L flask was evacuated and back-flushed with nitrogen, which was repeated 5 times. The mixture was heated at 100 °C for 18 h. The mixture was filtered through Celite, washing with EtOAc (500 mL). The filtrate was concentrated in vacuo. The residue was partitioned between EtOAc (700 mL) and brine (300 mL). The organic was extracted with EtOAc (200 mL). The combined organic was dried over Na₂SO₄, filtered, and concentrated in vacuo. The residue was dissolved in CH₂Cl₂ and split into seven equal portions. Each portion was absorbed onto a dryload cartridge immediately prior to chromatography. Purification was done on 120 g silica gel cartridges using gradient elution of 1% EtOAc in hexane to 40% EtOAc in hexane. The combined product fractions were concentrated in vacuo to give a waxy cake, which was broken up and dried under vacuum at room temperature for 20 h to give the product 1,1-dimethylethyl 5-(4,4,5,5-tetramethyl-1,3,2-dioxaborolan-2-yl)-2,3-dihydro-1H-indole-1-carboxylate (**4a**) (30.54 g, 82%) as a light yellow waxy solid. LC-MS (ES) $m/z = 346 [M + H]^+$, prominent fragment at 290 [$M - ^t\text{Bu}^+$]. ¹H NMR (400 MHz, DMSO-*d*₆) 1.27 (s, 12 H), 1.50 (s, 9 H), 3.05 (t, $J = 8.6$ Hz, 2 H), 3.91 (t, $J = 8.7$ Hz, 2 H), 7.43–7.52 (m, 2 H), 7.58–7.80 (br s, 1 H).

5-Bromothieno[2,3-*d*]pyrimidin-4-amine (7). A suspension of 5-bromo-4-chlorothieno[2,3-*d*]pyrimidine (1 g, 4.01 mmol) in concentrated aqueous ammonium hydroxide (150 mL) was stirred overnight at 90 °C in a sealed steel vessel. The mixture was allowed to cool to room temperature and filtered. The white solid in the filter was

air-dried to afford 5-bromothieno[2,3-*d*]pyrimidin-4-amine (796 mg, 86%). ¹H NMR (400 MHz, DMSO-*d*₆) 8.32 (s, 1 H), 7.78 (s, 1 H), 6.38–8.22 (broad s, 2H). LC–MS (ES) *m/z* = 229.9, 231.9 [M + H]⁺.

5-Bromo-7-methyl-7H-pyrrolo[2,3-*d*]pyrimidin-4-amine (10). To 4-chloro-1H-pyrrolo[2,3-*d*]pyrimidine (15.2 g, 99 mmol) in DMF (100 mL) at 0 °C was added 60% NaH (5.15 g, 129 mmol) portionwise. After H₂ bubbling stopped, iodomethane (6.81 mL, 109 mmol) was added dropwise, and then the reaction mixture was allowed to warm to room temperature. After 3 h, the reaction mixture was poured slowly onto water (~800 mL) (Caution: H₂ evolution due to quenching excess NaH). The resulting solid was filtered, washed with water followed by hexanes, and dried to afford 4-chloro-7-methyl-7H-pyrrolo[2,3-*d*]pyrimidine (12.2 g, 74%) as an off-white solid. ¹H NMR (400 MHz, DMSO-*d*₆) 8.64 (s, 1 H), 7.73 (d, *J* = 3.5 Hz, 1 H), 6.63 (d, *J* = 3.5 Hz, 1 H), 3.85 (s, 3 H). LC–MS (ES) *m/z* = 168.0, 170.0 [M + H]⁺.

To 4-chloro-7-methyl-7H-pyrrolo[2,3-*d*]pyrimidine (12.15 g, 72.5 mmol) in CH₂Cl₂ (200 mL) was added NBS (13.55 g, 76 mmol) portionwise, and the reaction mixture was stirred overnight at room temperature. The solvent was evaporated, and the solid was washed with water and dried to afford 5-bromo-4-chloro-7-methyl-7H-pyrrolo[2,3-*d*]pyrimidine (17 g, 95%) as an off-white solid. ¹H NMR (400 MHz, DMSO-*d*₆) 8.67 (s, 1 H), 7.99 (s, 1 H), 3.83 (s, 3 H). LC/MS (ES) *m/z* = 245.9, 247.9, 248.9, 249.9 [M + H]⁺.

A suspension of 5-bromo-4-chloro-7-methyl-7H-pyrrolo[2,3-*d*]pyrimidine (17 g, 69.0 mmol) in concentrated aqueous ammonium hydroxide (150 mL) was stirred for 2 days at 100 °C in a sealed vessel. The mixture was allowed to cool to room temperature and filtered. The collected solid was washed with Et₂O and dried to afford 5-bromo-7-methyl-7H-pyrrolo[2,3-*d*]pyrimidin-4-amine (12.5 g, 80%) as a white solid. ¹H NMR (400 MHz, DMSO-*d*₆) 8.11 (s, 1 H), 7.40 (s, 1 H), 6.73 (br s, 2 H), 3.67 (s, 3 H). LC–MS (ES) *m/z* = 228.9, 229.9 [M + H]⁺.

3-[1-(Phenylacetyl)-2,3-dihydro-1H-indol-5-yl]thieno[3,2-*c*]pyridin-4-amine (22). To a mixture of phenylacetic acid (0.687 g, 5.05 mmol) and HATU (2.112 g, 5.55 mmol) in DMF (5 mL) was added DIPEA (0.882 mL, 5.05 mmol), and the resulting mixture was stirred for 15 min at room temperature. 5-Bromo-2,3-dihydro-1H-indole (1 g, 5.05 mmol) was added, and the reaction mixture was stirred at room temperature overnight. The mixture was poured onto water, and the resulting precipitate was filtered and air-dried to afford the 5-bromo-1-(phenylacetyl)-2,3-dihydro-1H-indole (1.24 g, 78%) as a tan solid. LC–MS (ES) *m/z* = 338.0, 340.0 [M + Na]⁺. ¹H NMR (400 MHz, DMSO-*d*₆) 7.98 (d, *J* = 8.6 Hz, 1 H), 7.42 (s, 1 H), 7.19–7.37 (m, 6 H), 4.18 (t, *J* = 8.6 Hz, 2 H), 3.84 (s, 2 H), 3.16 (t, 2 H).

To 5-bromo-1-(phenylacetyl)-2,3-dihydro-1H-indole (0.658 g, 2.081 mmol), bispinacolatodiboron (0.634 g, 2.497 mmol), and potassium acetate (0.613 g, 6.24 mmol) in a sealable tube was added 1,4-dioxane (15 mL), and the mixture was degassed with N₂ for 10 min. PdCl₂(dppf)–CH₂Cl₂ adduct (0.085 g, 0.104 mmol) was added, and the reaction mixture was sealed and stirred for 48 h at 100 °C. The mixture was cooled to room temperature and treated with 5 mL of water, 3-bromothieno[3,2-*c*]pyridin-4-amine (0.524 g, 2.289 mmol), and NaHCO₃ (175 mg). The mixture was degassed with N₂ for 10 min. PdCl₂(dppf)–CH₂Cl₂ adduct (0.085 g, 0.104 mmol) was added, and the reaction mixture was sealed and stirred overnight at 100 °C. The mixture was poured onto water and ethyl acetate and then filtered. The filtrate was transferred to a separatory funnel. The organic layer was separated, and the aqueous layer was further extracted with ethyl acetate. The combined organic layers were washed with brine, dried (MgSO₄), filtered, and concentrated. Flash chromatography on SiO₂ (gradient 100% CHCl₃ to 90:10:1 CHCl₃/CH₃OH/NH₄OH) afforded a few fractions containing the desired product with an impurity. The fractions were combined and evaporated. The resulting residue was dissolved in MeOH/CH₂Cl₂ (1 mL/5 mL), dry loaded onto silica, and purified by chromatography (Analoxig 25–14 g cartridge) using a gradient of 0–100% EtOAc/hexane. The fractions with the pure compound were combined, the solvents were evaporated, and the resulting residue was triturated with EtOAc to give 3-[1-(phenylacetyl)-2,3-dihydro-1H-indol-5-yl]thieno[3,2-*c*]-

pyridin-4-amine (22) as an off-white solid (280 mg, 35%). ¹H NMR (400 MHz, DMSO-*d*₆) 8.16 (d, *J* = 8.3 Hz, 1 H), 7.82 (d, *J* = 5.6 Hz, 1 H), 7.41 (s, 1 H), 7.19–7.38 (m, 8 H), 5.41 (br s, 2 H), 4.25 (t, *J* = 8.6 Hz, 2 H), 3.89 (s, 2 H), 3.23 (t, 2 H). LC–MS (ES) *m/z* = 386.0 [M + H]⁺.

3-[1-(Phenylacetyl)-2,3-dihydro-1H-indol-5-yl]-7-(3-pyridinyl)thieno[3,2-*c*]pyridin-4-amine (2). To a solution of 3-[1-(phenylacetyl)-2,3-dihydro-1H-indol-5-yl]thieno[3,2-*c*]pyridin-4-amine (22) (150 mg, 0.389 mmol) in DMF (3.0 mL) cooled in an ice-bath was added NIS (96 mg, 0.428 mmol). The reaction mixture was stirred at room temperature overnight. Water was poured into the mixture. The formed brown solid was filtered and dried to give 185 mg (93%) of the product 7-iodo-3-[1-(phenylacetyl)-2,3-dihydro-1H-indol-5-yl]thieno[3,2-*c*]pyridin-4-amine (17), which was used without further purification. LC–MS (ES) *m/z* = 511.9 [M + H]⁺.

A 25 mL pressure tube was charged with 7-iodo-3-[1-(phenylacetyl)-2,3-dihydro-1H-indol-5-yl]thieno[3,2-*c*]pyridin-4-amine (182 mg, 0.356 mmol), 3-pyridinylboronic acid (43.7 mg, 0.356 mmol), [1,1'-bis(diphenylphosphino)ferrocene]palladium(II) dichloride dichloromethane complex (14.53 mg, 0.018 mmol), and sodium carbonate (75 mg, 0.712 mmol) followed by dioxane (5 mL) and water (1 mL). The mixture was heated at 120 °C for 30 min in a microwave reactor. Water (20 mL) and ethyl acetate (20 mL) were added, and the layers were separated. The organic layer was washed with brine, concentrated and the residue purified by silica gel chromatography (0–100% EtOAc in hexanes) to afford 3-[1-(phenylacetyl)-2,3-dihydro-1H-indol-5-yl]-7-(3-pyridinyl)thieno[3,2-*c*]pyridin-4-amine (2) (85 mg, 51%) as a gray solid. ¹H NMR (400 MHz, DMSO-*d*₆) 8.88 (d, *J* = 1.8 Hz, 1 H), 8.62 (dd, *J* = 4.8, 1.5 Hz, 1 H), 8.18 (d, *J* = 8.1 Hz, 1 H), 8.10 (dt, *J* = 8.1, 1.9 Hz, 1 H), 7.96 (s, 1 H), 7.56 (dd, *J* = 8.1, 4.8 Hz, 1 H), 7.50 (s, 1 H), 7.23–7.40 (m, 7 H), 5.63 (br s, 2 H), 4.26 (t, *J* = 8.5 Hz, 2 H), 3.90 (s, 2 H), 3.24 (t, 2 H). LC–MS (ES) *m/z* = 463.1 [M + H]⁺.

3-[1-(Phenylacetyl)-2,3-dihydro-1H-indol-5-yl]-7-(4-pyridinyl)thieno[3,2-*c*]pyridin-4-amine (18). A mixture of 7-iodo-3-[1-(phenylacetyl)-2,3-dihydro-1H-indol-5-yl]thieno[3,2-*c*]pyridin-4-amine (101 mg, 0.198 mmol), pyridine-4-boronic acid pinacol ester (53 mg, 0.258 mmol), and PdCl₂(dppf)–CH₂Cl₂ adduct (8 mg, 9.80 μmol) in 1,4-dioxane (1.5 mL) and saturated aqueous sodium bicarbonate (0.6 mL, 0.600 mmol) was degassed with nitrogen for 10 min in a microwave vial. The vial was then capped, and the mixture was stirred at 120 °C in the microwave for 30 min. The mixture was cooled, poured into water (15 mL), and extracted with ethyl acetate (2 × 15 mL). The combined extracts were washed with brine (1 × 15 mL), dried (Na₂SO₄), filtered, and concentrated in vacuo. The residue was purified by flash chromatography (Analoxig, 24 g SiO₂ cartridge), eluting with 25–100% EtOAc in hexanes gradient over 30 min, then EtOAc for 10 min, then 0–10% MeOH in EtOAc over 20 min to give 3-[1-(phenylacetyl)-2,3-dihydro-1H-indol-5-yl]-7-(4-pyridinyl)thieno[3,2-*c*]pyridin-4-amine (18) (66 mg, 69% yield) as a beige solid. LC/MS (ES) *m/z* = 463 [M + H]⁺. ¹H NMR (400 MHz, DMSO-*d*₆) 3.24 (t, *J* = 8.46 Hz, 2 H), 3.90 (s, 2 H), 4.26 (t, *J* = 8.46 Hz, 2 H), 5.74 (br s, 2 H), 7.23–7.39 (m, 7 H), 7.52 (s, 1 H), 7.70–7.75 (m, 2 H), 8.09 (s, 1 H), 8.18 (d, *J* = 8.34 Hz, 0 H), 8.65–8.72 (m, 2 H).

3-[1-(Phenylacetyl)-2,3-dihydro-1H-indol-5-yl]-7-(4-piperidinyl)thieno[3,2-*c*]pyridin-4-amine (19). A mixture of 7-iodo-3-[1-(phenylacetyl)-2,3-dihydro-1H-indol-5-yl]thieno[3,2-*c*]pyridin-4-amine (298 mg, 0.583 mmol), 3,6-dihydro-2H-pyridine-1-*N*-Boc-4-boronic acid pinacol ester (238 mg, 0.770 mmol), and PdCl₂(dppf)–CH₂Cl₂ adduct (24 mg, 0.029 mmol) in 1,4-dioxane (6 mL) and saturated aqueous sodium bicarbonate (2 mL, 2.0 mmol) was degassed with nitrogen for 10 min in a microwave vial. The vial was then capped, and the mixture was stirred at 120 °C in a microwave reactor for 30 min. LC–MS showed complete conversion to the product. The mixture was cooled, poured into water (50 mL), and extracted with ethyl acetate (2 × 50 mL). The extracts were washed with brine (1 × 75 mL), dried (Na₂SO₄), filtered, and concentrated in vacuo. The residue was purified by flash chromatography (Analoxig, 40 g SiO₂, 25–100% EtOAc in hexanes gradient over 45 min, then EtOAc for 5 min) to give 1,1-dimethylethyl 4-{4-amino-3-[1-(phenylacetyl)-

2,3-dihydro-1*H*-indol-5-yl]thieno[3,2-*c*]pyridin-7-yl]-3,6-dihydro-1(2*H*)-pyridinecarboxylate (280 mg, 85%) as a beige solid. LC/MS (ES) $m/z = 567 [M + H]^+$.

A solution of 1,1-dimethylethyl 4-{4-amino-3-[1-(phenylacetyl)-2,3-dihydro-1*H*-indol-5-yl]thieno[3,2-*c*]pyridin-7-yl]-3,6-dihydro-1(2*H*)-pyridinecarboxylate (220 mg, 0.388 mmol), ethanol (10 mL), and THF (15 mL) was subjected to 10% Pd/C hydrogenation on an H-Cube reactor at 40 °C and 40 bar for 23 h. After concentration in vacuo, and the residue was dry loaded onto silica gel (1 g) and purified by flash chromatography (Analogix, 40 g SiO₂, CH₂Cl₂ to 95/5/0.5 CH₂Cl₂/MeOH/NH₄OH gradient over 42 min) to give 1,1-dimethylethyl 4-{4-amino-3-[1-(phenylacetyl)-2,3-dihydro-1*H*-indol-5-yl]thieno[3,2-*c*]pyridin-7-yl]-1-piperidinecarboxylate (91 mg, 41%) as an off-white solid. LC/MS (ES) $m/z = 569.2 [M + H]^+$.

TFA (0.5 mL, 6.49 mmol) was added to a suspension of 1,1-dimethylethyl 4-{4-amino-3-[1-(phenylacetyl)-2,3-dihydro-1*H*-indol-5-yl]thieno[3,2-*c*]pyridin-7-yl]-1-piperidinecarboxylate (90 mg, 0.158 mmol) in CH₂Cl₂ (3.5 mL), and the mixture was stirred at room temperature under nitrogen for 30 min. The reaction mixture was then concentrated in vacuo. The residue was taken up in CH₂Cl₂ and passed through a PL-HCO₃ MP-resin cartridge, rinsing with more CH₂Cl₂. The filtrate was concentrated in vacuo, and the residue was purified by flash chromatography (Analogix, 24 g SiO₂, CH₂Cl₂ to 80/20/2 CH₂Cl₂/MeOH/NH₄OH gradient over 30 min) to give 3-[1-(phenylacetyl)-2,3-dihydro-1*H*-indol-5-yl]-7-(4-piperidinyl)thieno[3,2-*c*]pyridin-4-amine (19) (37 mg, 47%) as a white solid. LC-MS (ES) $m/z = 469 [M + H]^+$. ¹H NMR (400 MHz, DMSO-*d*₆) 1.64–1.77 (m, 2 H), 1.77–1.86 (m, 2 H), 2.57–2.77 (m, 3 H), 3.07 (d, *J* = 12.13 Hz, 2 H), 3.22 (t, *J* = 8.34 Hz, 2 H), 3.89 (s, 2 H), 4.24 (t, *J* = 8.59 Hz, 2 H), 5.24 (br s, 2 H), 7.19–7.39 (m, 7 H), 7.41 (s, 1 H), 7.70 (s, 1 H), 8.15 (d, *J* = 8.34 Hz, 1 H).

3-[1-(Phenylacetyl)-2,3-dihydro-1*H*-indol-5-yl]-7-(1*H*-pyrazol-4-yl)thieno[3,2-*c*]pyridin-4-amine (20). A mixture of 7-iodo-3-[1-(phenylacetyl)-2,3-dihydro-1*H*-indol-5-yl]thieno[3,2-*c*]pyridin-4-amine (101 mg, 0.198 mmol), 1-Boc-pyrazol-4-boronic acid pinacol ester (88 mg, 0.299 mmol), and PdCl₂(dppf)-CH₂Cl₂ adduct (9 mg, 0.011 mmol) in 1,4-dioxane (2 mL) and saturated aqueous sodium bicarbonate (0.6 mL, 0.600 mmol) was degassed with nitrogen for 10 min in a microwave vial. The vial was then capped, and the mixture was stirred at 120 °C in a microwave reactor for 30 min. The mixture was cooled, poured into water (15 mL), and extracted with ethyl acetate (2 × 15 mL). The combined extracts were washed with brine (1 × 15 mL), dried (Na₂SO₄), filtered, and concentrated in vacuo. The residue was purified by flash chromatography (Analogix, 24 g SiO₂, 50–100% EtOAc in hexanes gradient over 15 min, then EtOAc for 5 min, then 0–10% MeOH in EtOAc over 20 min) to give 3-[1-(phenylacetyl)-2,3-dihydro-1*H*-indol-5-yl]-7-(1*H*-pyrazol-4-yl)thieno[3,2-*c*]pyridin-4-amine (20) (50 mg, 53%) as a light gray solid. LC-MS (ES) $m/z = 452 [M + H]^+$. ¹H NMR (400 MHz, DMSO-*d*₆) 3.24 (t, *J* = 8.34 Hz, 2 H), 3.89 (s, 2 H), 4.26 (t, *J* = 8.46 Hz, 2 H), 5.40 (br s, 2 H), 7.22–7.30 (m, 2 H), 7.30–7.40 (m, 5 H), 7.48 (s, 1 H), 7.95 (br s, 1 H), 8.06 (s, 1 H), 8.12–8.21 (m, 2 H), 13.10 (br s, 1 H).

7-(1-Methyl-1*H*-pyrazol-4-yl)-3-[1-(phenylacetyl)-2,3-dihydro-1*H*-indol-5-yl]thieno[3,2-*c*]pyridin-4-amine (21). A mixture of 7-iodo-3-[1-(phenylacetyl)-2,3-dihydro-1*H*-indol-5-yl]thieno[3,2-*c*]pyridin-4-amine (102 mg, 0.199 mmol), 1-methylpyrazole-4-boronic acid pinacol ester (60 mg, 0.288 mmol), and PdCl₂(dppf)-CH₂Cl₂ adduct (8 mg, 9.80 μmol) in 1,4-dioxane (2.0 mL) and saturated aqueous sodium bicarbonate (0.6 mL, 0.600 mmol) was degassed with nitrogen for 10 min in a microwave vial. The vial was then capped, and the mixture was stirred at 120 °C in a microwave reactor for 30 min. The mixture was cooled, poured into water (15 mL), and extracted with ethyl acetate (2 × 15 mL). The extracts were washed with brine (1 × 15 mL), dried (Na₂SO₄), filtered, and concentrated in vacuo. The residue was purified by flash chromatography (Analogix, 24 g SiO₂, 50–100% EtOAc in hexanes gradient over 10 min, then EtOAc for 5 min, then 0–10% MeOH in EtOAc over 20 min) to give 7-(1-methyl-1*H*-pyrazol-4-yl)-3-[1-(phenylacetyl)-2,3-dihydro-1*H*-indol-5-yl]thieno[3,2-*c*]pyridin-4-amine (21) (69 mg, 71%) as a light gray solid. LC-MS (ES) $m/z = 466 [M + H]^+$. ¹H NMR (400 MHz, DMSO-*d*₆)

3.24 (t, *J* = 8.46 Hz, 2 H), 3.89 (s, 2 H), 3.93 (s, 3 H), 4.26 (t, *J* = 8.46 Hz, 2 H), 5.41 (br s, 2 H), 7.22–7.30 (m, 2 H), 7.30–7.39 (m, 5 H), 7.49 (s, 1 H), 7.88 (s, 1 H), 8.03 (s, 1 H), 8.14 (s, 1 H), 8.17 (d, *J* = 8.08 Hz, 1 H).

3-[1-(Phenylacetyl)-2,3-dihydro-1*H*-indol-5-yl]thieno[3,2-*c*]pyridin-4-amine (22). A sealable tube was charged with 5-bromo-1-(phenylacetyl)-2,3-dihydro-1*H*-indole (0.658 g, 2.081 mmol), bispinacolatodiboron (0.634 g, 2.5 mmol), and potassium acetate (0.613 g, 6.24 mmol). 1,4-Dioxane (15 mL) was added, and the mixture was degassed with N₂ for 10 min. PdCl₂(dppf)-CH₂Cl₂ adduct (0.085 g, 0.104 mmol) was added, and the reaction mixture was stirred for 48 h at 100 °C. The mixture was cooled to room temperature and treated with 5 mL of water, 3-bromothieno[3,2-*c*]pyridin-4-amine (0.524 g, 2.289 mmol), and NaHCO₃ (175 mg). The mixture was degassed with N₂ for 10 min. PdCl₂(dppf)-CH₂Cl₂ adduct (0.085 g, 0.104 mmol) was added, and the reaction mixture was stirred overnight at 100 °C. The mixture was poured onto water and ethyl acetate and was filtered. The filtrate was transferred to a separatory funnel. The organic layer was separated, and the aqueous layer was further extracted with ethyl acetate. The combined organic layers were washed with brine, dried (MgSO₄), filtered, and concentrated. Flash chromatography on SiO₂ (gradient 100% CHCl₃ to 90:10:1 CHCl₃/CH₃OH/NH₄OH) afforded a few fractions containing the desired product with an impurity. The fractions were combined and evaporated. The resulting residue was dissolved in MeOH/CH₂Cl₂ (1 mL/5 mL), then dry loaded and purified by silica gel chromatography (Analogix 25–14 g cartridge), using a gradient of 0–100% EtOAc/hexane. The fractions with the pure compound were combined and evaporated. The resulting residue was triturated with EtOAc to give 3-[1-(phenylacetyl)-2,3-dihydro-1*H*-indol-5-yl]thieno[3,2-*c*]pyridin-4-amine (22) as an off-white solid (280 mg, 35%). LC-MS (ES) $m/z = 386.0 [M + H]^+$. ¹H NMR (400 MHz, DMSO-*d*₆) 8.16 (d, *J* = 8.3 Hz, 1 H), 7.82 (d, *J* = 5.6 Hz, 1 H), 7.41 (s, 1 H), 7.19–7.38 (m, 8 H), 5.41 (br s, 2 H), 4.25 (t, *J* = 8.6 Hz, 2 H), 3.89 (s, 2 H), 3.23 (t, 2 H).

3-[1-[(2,5-Difluorophenyl)acetyl]-2,3-dihydro-1*H*-indol-5-yl]thieno[3,2-*c*]pyridin-4-amine (23). To a mixture of (2,5-difluorophenyl)acetic acid (0.869 g, 5.05 mmol) and HATU (2.11 g, 5.55 mmol) in DMF (10 mL) was added DIPEA (0.882 mL, 5.05 mmol), and the resulting mixture was stirred for 15 min at room temperature. 5-Bromo-2,3-dihydro-1*H*-indole (1 g, 5.05 mmol) was added, and the reaction mixture was stirred at room temperature for 1 h. The mixture was poured onto water, and the resulting aqueous mixture was filtered to afford 5-bromo-1-[(2,5-difluorophenyl)acetyl]-2,3-dihydro-1*H*-indole (1.6 g) as a tan solid. LC-MS (ES) $m/z = 376, 378 [M + Na]^+$. ¹H NMR (400 MHz, DMSO-*d*₆) 7.93 (d, *J* = 8.6 Hz, 1 H), 7.45 (s, 1 H), 7.32 (dd, *J* = 8.6, 1.8 Hz, 1 H), 7.12–7.29 (m, 3 H), 4.24 (t, *J* = 8.5 Hz, 2 H), 3.91 (s, 2 H), 3.21 (t, 2 H).

In a sealable tube, to 5-bromo-1-[(2,5-difluorophenyl)acetyl]-2,3-dihydro-1*H*-indole (0.700 g, 1.99 mmol), bispinacolatodiboron (0.606 g, 2.39 mmol), and potassium acetate (0.585 g, 5.96 mmol) was added 1,4-dioxane (15 mL), and the mixture was degassed with N₂ for 10 min. PdCl₂(dppf)-CH₂Cl₂ adduct (0.081 g, 0.99 mmol) was added, and the reaction mixture was sealed and stirred for 48 h at 100 °C. The mixture was cooled to room temperature and treated with 5 mL of water, 3-bromothieno[3,2-*c*]pyridin-4-amine (0.501 g, 2.186 mmol), and sodium bicarbonate (167 mg, 1.988 mmol). The mixture was degassed with N₂ for 10 min. PdCl₂(dppf)-CH₂Cl₂ adduct (0.085 g, 0.104 mmol) was added, and the reaction mixture was stirred overnight at 100 °C. The mixture was poured onto water and ethyl acetate, then filtered. The filtrate was transferred to a separatory funnel, and the organic layer was separated. The aqueous layer was further extracted with ethyl acetate, and the combined organic layers were washed with brine, dried (MgSO₄), filtered, and concentrated. Purification by chromatography (Analogix silica gel cartridge), eluting with a gradient of 0–100% EtOAc/hexane, gave 526 mg (62%) of 3-[1-[(2,5-difluorophenyl)acetyl]-2,3-dihydro-1*H*-indol-5-yl]thieno[3,2-*c*]pyridin-4-amine (23) as an off-white solid. LC-MS (ES) $m/z = 422.2 [M + H]^+$. ¹H NMR (400 MHz, DMSO-*d*₆) 8.11 (d, *J* = 8.3 Hz, 1 H), 7.82 (d, *J* = 5.6 Hz, 1 H), 7.42 (s, 1 H), 7.35 (s, 1 H), 7.12–7.31

(m, 5 H), 5.41 (br s, 2 H), 4.31 (t, $J = 8.3$ Hz, 2 H), 3.96 (s, 2 H), 3.23–3.31 (m, 2 H).

5-{1-[(2,5-Difluorophenyl)acetyl]-2,3-dihydro-1H-indol-5-yl}-thieno[2,3-d]pyrimidin-4-amine (24). To a mixture of 5-bromo-1-[(2,5-difluorophenyl)acetyl]-2,3-dihydro-1H-indole (150 mg, 0.426 mmol), bis(pinacolato)diboron (114 mg, 0.447 mmol), and potassium acetate (125 mg, 1.278 mmol) was added 1,4-dioxane (6 mL), and the mixture was degassed with N_2 for 10 min. $PdCl_2(dppf)-CH_2Cl_2$ adduct (17.39 mg, 0.021 mmol) was added, and the reaction mixture was stirred for 3 h at 100 °C in a sealed vessel. The mixture was cooled to room temperature. 5-Bromothieno[2,3-d]pyrimidin-4-amine (7) (103 mg, 0.447 mmol) and saturated aqueous $NaHCO_3$ (2 mL) were added, and N_2 gas was bubbled through the mixture for 10 min. $PdCl_2(dppf)-CH_2Cl_2$ adduct (17.39 mg, 0.021 mmol) was added. The vessel was sealed, and the reaction mixture was stirred overnight at 100 °C. The mixture was poured onto water, and a precipitate was formed. The mixture was filtered, and the solid was taken up into a mixture of 20% CH_3OH/CH_2Cl_2 . The resulting mixture was filtered, injected into a 90 g silica gel column, and purified via flash chromatography (gradient 100% hexanes to 100% EtOAc). The fractions containing the product were combined and concentrated to afford a solid. Trituration with Et_2O afforded 5-{1-[(2,5-difluorophenyl)acetyl]-2,3-dihydro-1H-indol-5-yl}thieno[2,3-d]pyrimidin-4-amine (120 mg, 67%) as a white solid. 1H NMR (400 MHz, $DMSO-d_6$) 3.27 (t, 2 H), 3.96 (s, 2 H), 4.31 (t, $J = 8.46$ Hz, 2 H), 7.13–7.32 (m, 4 H), 7.37 (s, 1 H), 7.43 (s, 1 H), 8.11 (d, $J = 8.08$ Hz, 1 H), 8.34 (s, 1 H). LC–MS (ES) $m/z = 423.1 [M + H]^+$.

5-{1-[(2,5-Difluorophenyl)acetyl]-2,3-dihydro-1H-indol-5-yl}-furo[2,3-d]pyrimidin-4-amine (25). To a suspension of 1,5-diacetylindoline (10.0 g, 49.2 mmol) in 90 mL of THF at room temperature was added pyridinium tribromide (16.52 g, 51.7 mmol, 1 equiv) as a solid portionwise over a period of 10 min. When there was about 1.5 g of pyridinium tribromide left, the mixture solidified. Another 30 mL of THF was added so that the mixture could be stirred. The remaining 1.5 g of tribromide was added in one portion, and the mixture was stirred at room temperature. After 1.5 h, LC–MS showed complete conversion. The suspension was filtered, and the cake was washed with THF (2×30 mL) and then water (2×50 mL). The wet cake was dried under house vacuum at room temperature for 2 days to give 1-(1-acetyl-2,3-dihydro-1H-indol-5-yl)-2-bromoethanone (12.89 g, 93%) as light gray solids. LC–MS (ES) $m/z = 281.9$, 283.9. 1H NMR (400 MHz, $DMSO-d_6$, * denotes minor rotamer signal) 2.14–2.27 (m, 3 H), 3.20 (t, $J = 8.5$ Hz, 2 H), 4.17 (t, $J = 8.5$ Hz, 2 H), 4.84, 5.86* (s, 2H), 7.78–7.94 (m, 2 H), 8.05–8.18 (m, 1H).

A pasty suspension of 1-(1-acetyl-2,3-dihydro-1H-indol-5-yl)-2-bromoethanone (39.0 g, 138 mmol) and sodium acetate (56.7 g, 691 mmol, 5 equiv) in EtOH (300 mL) and water (300 mL) was heated in an oil bath at 70 °C for 3 h. The mixture was cooled in an ice bath and then stored in the refrigerator overnight. To the cold suspension was added cold 6 N NaOH (25 mL, 150 mmol, 1.09 equiv). The mixture was stirred in an ice bath for 2.5 h, and the cold mixture was acidified with 2 N HCl to pH 6. The mixture was concentrated in vacuo to about 100 mL of volume as an aqueous slurry, which was diluted with 200 mL of water and ether (300 mL). The suspension was stirred at room temperature for 15 min, then filtered. The light brownish cake was washed with water (2×100 mL) and dried under house vacuum overnight to give 1-(1-acetyl-2,3-dihydro-1H-indol-5-yl)-2-hydroxyethanone (14) (24.22 g, 80%). LC–MS (ES) $m/z = 220.1 [M + H]^+$. 1H NMR (400 MHz, $DMSO-d_6$) 8.10 (d, $J = 8.8$ Hz, 1 H), 7.66–7.88 (m, 2 H), 4.97 (t, $J = 5.8$ Hz, 1 H), 4.73 (d, $J = 5.8$ Hz, 2 H), 4.16 (t, $J = 8.5$ Hz, 2 H), 3.19 (t, $J = 8.6$ Hz, 2 H), 2.20 (s, 3 H).

To a suspension of 1-(1-acetyl-2,3-dihydro-1H-indol-5-yl)-2-hydroxyethanone (2.29 g, 10.45 mmol) and malononitrile (759 mg, 11.49 mmol, 1.1 equiv) in DMF (16 mL) at room temperature was added diethylamine (1.64 mL, 15.67 mmol, 1.5 equiv). The brown suspension was stirred at ambient temperature for 2 h, during which it became a solution and then a suspension again. The mixture was poured into 150 mL of water, then filtered. The cake was washed with

water and dried under house vacuum overnight to give 4-(1-acetyl-2,3-dihydro-1H-indol-5-yl)-2-amino-3-furancarboxitrile (15) (2.22 g, 80%) as beige solids. LC–MS (ES) $m/z = 268 [M + H]^+$. 1H NMR (400 MHz, methanol- d_4) 8.11 (d, $J = 8.3$ Hz, 1 H), 7.46 (s, 1 H), 7.40 (d, $J = 8.3$ Hz, 1 H), 7.10 (s, 1 H), 4.18 (t, $J = 8.5$ Hz, 2 H), 3.25 (t, $J = 8.5$ Hz, 2 H), 2.26 (s, 3 H).

To a suspension of 4-(1-acetyl-2,3-dihydro-1H-indol-5-yl)-2-amino-3-furancarboxitrile (1.248 g, 4.67 mmol) in 1,4-dioxane (12 mL) was added bis(ethoxy)methyl acetate (2 mL, 12.29 mmol, 2.63 equiv) in one portion. The resulting suspension was heated in an oil bath at 60 °C. After 15 min of heating, the mixture became a solution. Heating was continued for 4 h, and the mixture was cooled to room temperature. After 10 h of aging at room temperature, the mixture became a suspension, which was filtered. The cake was washed with hexane and dried under vacuum to give ethyl [4-(1-acetyl-2,3-dihydro-1H-indol-5-yl)-3-cyano-2-furanyl]imidoformate (1.20 g, 76%) as tan solids. 1H NMR (400 MHz, $DMSO-d_6$) 1.34 (t, $J = 7.1$ Hz, 3 H), 2.18 (s, 3 H), 3.19 (t, $J = 8.6$ Hz, 2 H), 4.14 (t, $J = 8.6$ Hz, 2 H), 4.38 (q, $J = 6.6$ Hz, 2 H), 7.38–7.47 (m, 1 H), 7.49 (s, 1 H), 7.94 (s, 1 H), 8.09 (d, $J = 8.3$ Hz, 1 H), 8.64 (s, 1 H).

To a homogeneous dark brown solution of ethyl [4-(1-acetyl-2,3-dihydro-1H-indol-5-yl)-3-cyano-2-furanyl]imidoformate (2.34 g, 7.24 mmol) in 20 mL of CH_2Cl_2 was added 6 mL of 7 N NH_3 in MeOH in one portion. The resulting mixture was stirred at room temperature. After 10 min, the mixture became a suspension. After 18 h, LC–MS showed conversion complete. The suspension was concentrated in vacuo, and the residue was dried under vacuum to give 5-(1-acetyl-2,3-dihydro-1H-indol-5-yl)furo[2,3-d]pyrimidin-4-amine (16) (1.92 g, 90% yield) as a beige solid. LC–MS (ES) $m/z = 294.9 [M + H]^+$. 1H NMR (400 MHz, $DMSO-d_6$) 8.20 (br s, 2 H), 8.06 (d, $J = 8.3$ Hz, 1 H), 7.87 (br s, 1 H), 7.64 (s, 1 H), 7.25–7.55 (m, 2 H), 4.12 (t, $J = 8.5$ Hz, 2 H), 3.11–3.26 (m, 2 H), 2.17 (s, 3 H); NH_2 protons not visible.

A dark brownish suspension of 5-(1-acetyl-2,3-dihydro-1H-indol-5-yl)furo[2,3-d]pyrimidin-4-amine (1.71 g, 5.81 mmol) and $LiOH \cdot H_2O$ (5.50 g, 131 mmol, 22.6 equiv) in 50 mL of EtOH and 10 mL of water and 10 mL of DMSO was degassed and back-flushed with nitrogen. This cycle was repeated 4X, and the mixture was heated in an oil bath at 100 °C for 48 h. LC–MS showed there was still 22% starting material left. To the mixture was added KOH (3.26 g, 58.1 mmol, 10 equiv) as pellets. The suspension was degassed and heated at 100 °C for another 16 h. The mixture was cooled and filtered. The cake was rinsed with 30 mL of EtOH, and the filtrate was cooled in an ice bath. The pH was adjusted by adding cold 6 N HCl to pH 7–8. The resulting brownish mixture was concentrated in vacuo to remove as much solvent as possible. The solid residue was taken up in water to give a suspension, which was chilled in a refrigerator, followed by filtration. The cake was washed with water (2×8 mL) and dried under house vacuum for 5 h and then under vacuum over P_2O_5 for 15 h to afford 5-(2,3-dihydro-1H-indol-5-yl)furo[2,3-d]pyrimidin-4-amine (0.76 g, 47%) as dark tan-colored solids. LC–MS (ES) $m/z = 252.9 [M + H]^+$. 1H NMR (400 MHz, $DMSO-d_6$) 8.23 (s, 1 H), 7.79 (s, 1 H), 7.16 (s, 1 H), 7.05 (dd, $J = 8.0, 1.6$ Hz, 1 H), 6.61 (d, $J = 7.8$ Hz, 1 H), 5.77 (s, 1 H), 3.48 (td, $J = 8.5, 1.6$ Hz, 2 H), 2.98 (t, 2 H); NH_2 protons not visible.

To a stirred dark brownish solution of 5-(2,3-dihydro-1H-indol-5-yl)furo[2,3-d]pyrimidin-4-amine (360 mg, 1.43 mmol) and HATU (597 mg, 1.57 mmol, 1.1 equiv) in 3 mL of DMF was added DIEA (274 μ L, 1.57 mmol, 1.1 equiv). To this mixture was added (2,5-difluorophenyl)acetic acid portionwise (246 mg total, 1.43 mmol, 1 equiv) over a 1 h period. The mixture was stirred for another 2 h and then added to 50 mL of ice–water. The resulting suspension was filtered. The brown cake was washed with water (2×10 mL) and then air-dried to give crude product (760 mg). This material was dissolved in 10% MeOH in CH_2Cl_2 and adsorbed onto silica. Purification was performed on a 60 g silica gel cartridge using gradient elution of 1% A to 55% A in CH_2Cl_2 (A was a mixture of 3200 mL of CH_2Cl_2 , 800 mL of MeOH, and 80 mL of concentrated NH_4OH). Pure fractions were combined and concentrated in vacuo. The residue was dissolved in 10% MeOH in $CHCl_3$ and filtered. The filtrate was concentrated in

vacuo, and the residue was taken up in 1.5 mL of CHCl₃. MTBE (1 mL) and hexane (7 mL) were added to give a suspension, which was filtered. The cake was washed with hexane (2 × 4 mL) and then dried under vacuum at 65 °C for 18 h to afford 5-[1-[(2,5-difluorophenyl)acetyl]-2,3-dihydro-1H-indol-5-yl]furo[2,3-d]pyrimidin-4-amine (25) (295 mg, 32%) as an off-white solid. LC-MS (ES) *m/z* = 407 [M + H]⁺. ¹H NMR (400 MHz, DMSO-*d*₆) 3.28 (t, *J* = 8.6 Hz, 2 H), 3.96 (s, 3 H), 4.30 (t, *J* = 8.5 Hz, 2 H), 7.13–7.28 (m, 3 H), 7.30 (d, *J* = 9.1 Hz, 1 H), 7.40 (s, 1 H), 7.93 (s, 1 H), 8.12 (d, *J* = 8.3 Hz, 1 H), 8.25 (s, 1 H); NH₂ protons not visible.

3-[1-[(2,5-Difluorophenyl)acetyl]-2,3-dihydro-1H-indol-5-yl]furo[3,2-*c*]pyridin-4-amine (26). A mixture of 3-bromofuro[3,2-*c*]pyridin-4-amine (8) (3.0 g, 14.09 mmol), 1,1-dimethylethyl 5-(4,4,5,5-tetramethyl-1,3,2-dioxaborolan-2-yl)-2,3-dihydro-1H-indole-1-carboxylate (4a) (5.35 g, 15.48 mmol), and PdCl₂(dppf)-CH₂Cl₂ adduct (0.573 g, 0.7 mmol) in 1,4-dioxane (120 mL) and saturated aqueous sodium bicarbonate (43 mL, 43.0 mmol) was degassed with nitrogen for 20 min. The mixture was then stirred at reflux under nitrogen for 16 h. It was then cooled, poured into half-saturated aqueous NaHCO₃ (250 mL), and extracted with ethyl acetate (2 × 250 mL). The combined extracts were washed with brine (1 × 250 mL), dried (Na₂SO₄), filtered, and concentrated in vacuo. The residue was purified by flash chromatography (Analogix, 400 g SiO₂, 20–100% EtOAc in hexanes gradient over 60 min, then 100% EtOAc for 15 min) to give 1,1-dimethylethyl 5-(4-aminofuro[3,2-*c*]pyridin-3-yl)-2,3-dihydro-1H-indole-1-carboxylate (3.93 g, 79%) as an off-white solid. LC-MS (ES) *m/z* = 352 [M + H]⁺. ¹H NMR (400 MHz, DMSO-*d*₆) 1.53 (s, 9 H), 3.14 (t, *J* = 8.59 Hz, 2 H), 3.97 (t, *J* = 8.72 Hz, 2 H), 5.52 (s, 2 H), 6.93 (d, *J* = 5.81 Hz, 1 H), 7.30 (d, *J* = 8.08 Hz, 1 H), 7.34 (s, 1 H), 7.83 (br s, 1 H), 7.86 (d, *J* = 5.81 Hz, 1 H), 7.89 (s, 1 H).

A mixture of 1,1-dimethylethyl 5-(4-aminofuro[3,2-*c*]pyridin-3-yl)-2,3-dihydro-1H-indole-1-carboxylate (1.04 g, 2.96 mmol) and HCl and 4.0 M in dioxane (15 mL, 60.0 mmol) was stirred at room temperature under nitrogen for 4.5 h. The reaction mixture was then concentrated in vacuo to give 3-(2,3-dihydro-1H-indol-5-yl)furo[3,2-*c*]pyridin-4-amine dihydrochloride (2HCl) (973 mg, 96% yield) as an off-white solid, which was used without further purification. LC-MS (ES) *m/z* = 252 [M + H]⁺. ¹H NMR (400 MHz, DMSO-*d*₆) 8.34 (s, 1 H), 8.06 (d, *J* = 7.1 Hz, 1 H), 7.60 (br s, 2 H), 7.49 (s, 1 H), 7.36–7.46 (m, 2 H), 7.30 (d, *J* = 7.8 Hz, 1 H), 4.65 (br s, 2 H), 3.70 (t, *J* = 8.1 Hz, 2 H), 3.20 (t, *J* = 8.0 Hz, 2 H).

A mixture of 3-(2,3-dihydro-1H-indol-5-yl)furo[3,2-*c*]pyridin-4-amine-2HCl (688 mg, 2.016 mmol), 2,5-difluorophenylacetic acid (354 mg, 2.057 mmol), HATU (844 mg, 2.220 mmol), and DIPEA (1.4 mL, 8.02 mmol) in DMF (15 mL) was stirred at room temperature for 17 h. HPLC indicated complete conversion, so the mixture was poured into water (75 mL), the suspension was stirred for about 10 min, and the precipitate was collected by vacuum filtration and dried by suction to give 3-[1-[(2,5-difluorophenyl)acetyl]-2,3-dihydro-1H-indol-5-yl]furo[3,2-*c*]pyridin-4-amine (26) (834 mg, 97% yield) as a tan solid. LC-MS (ES) *m/z* = 406 [M + H]⁺. ¹H NMR (400 MHz, DMSO-*d*₆) 3.29 (t, *J* = 8.34 Hz, 2 H), 3.96 (s, 2 H), 4.31 (t, *J* = 8.46 Hz, 2 H), 5.52 (s, 2 H), 6.93 (d, *J* = 5.81 Hz, 1 H), 7.14–7.34 (m, 4 H), 7.41 (s, 1 H), 7.87 (d, *J* = 5.81 Hz, 1 H), 7.92 (s, 1 H), 8.13 (d, *J* = 8.08 Hz, 1 H).

3-[1-[(2,5-Difluorophenyl)acetyl]-2,3-dihydro-1H-indol-5-yl]-1-methyl-1H-pyrazolo[3,4-*d*]pyrimidin-4-amine (27). To a mixture of 5-bromo-1-[(2,5-difluorophenyl)acetyl]-2,3-dihydro-1H-indole (160 mg, 0.454 mmol), bis(pinacolato)diboron (127 mg, 0.500 mmol), and potassium acetate (134 mg, 1.363 mmol) was added 1,4-dioxane (6 mL), and the mixture was degassed with N₂ for 10 min. PdCl₂(dppf)-CH₂Cl₂ adduct (18.55 mg, 0.023 mmol) was added, and the reaction mixture was stirred for 3 h at 100 °C in a sealed vessel. The mixture was cooled to room temperature. 3-Bromo-1-methyl-1H-pyrazolo[3,4-*d*]pyrimidin-4-amine (104 mg, 0.454 mmol) and saturated aqueous NaHCO₃ (2 mL) were added, and N₂ gas was bubbled through the mixture for 10 min. PdCl₂(dppf)-CH₂Cl₂ adduct (18.55 mg, 0.023 mmol) was added. The vessel was sealed, and the reaction mixture was stirred overnight at 100 °C. The mixture was

allowed to cool to room temperature and poured onto water (~150 mL). The resulting mixture was filtered, and the collected solid was triturated with Et₂O and then taken up in a 90:10 mixture of CHCl₃/CH₃OH (~7 mL), which was then filtered. The filtrate was injected into a 90 g SiO₂ column. Flash chromatography on SiO₂ (gradient 100% CHCl₃ to 90:10:1 CHCl₃/CH₃OH/NH₄OH) provided 3-[1-[(2,5-difluorophenyl)acetyl]-2,3-dihydro-1H-indol-5-yl]-1-methyl-1H-pyrazolo[3,4-*d*]pyrimidin-4-amine (27) (160 mg, 84%) as a brown solid. ¹H NMR (400 MHz, DMSO-*d*₆) 3.29 (t, *J* = 8.34 Hz, 2 H), 3.94 (s, 3 H), 3.97 (s, 2 H), 4.30 (t, *J* = 8.46 Hz, 2 H), 7.14–7.31 (m, 3 H), 7.44 (d, *J* = 8.34 Hz, 1 H), 7.53 (s, 1 H), 8.14 (d, *J* = 8.34 Hz, 1 H), 8.25 (s, 1 H). LC-MS (ES) *m/z* = 421.1 [M + H]⁺.

5-[1-[(2,5-Difluorophenyl)acetyl]-2,3-dihydro-1H-indol-5-yl]-7-methyl-7H-pyrrolo[2,3-*d*]pyrimidin-4-amine (28). A mixture of 5-bromo-7-methyl-7H-pyrrolo[2,3-*d*]pyrimidin-4-amine (10) (50.0 g, 220 mmol), 1,1-dimethylethyl 5-(4,4,5,5-tetramethyl-1,3,2-dioxaborolan-2-yl)-2,3-dihydro-1H-indole-1-carboxylate (95 g, 275 mmol, 1.25 equiv), Pd₂(dba)₃ (4.03 g, 4.40 mmol, 0.02 equiv), and K₃PO₄ monohydrate (101 g, 440 mmol, 2.0 equiv) in dioxane (750 mL) and water (250 mL) in a 2 L three-neck flask fitted with a condenser and an overhead stirrer was degassed and backflushed with nitrogen, followed by addition of tri(*tert*-butyl)phosphonium tetrafluoroborate (2.56 g, 8.81 mmol, 0.04 equiv). The mixture was degassed and backflushed with nitrogen 4 times. The mixture was heated at 85 °C for 90 min, and the hot mixture was filtered. The hot filtrate was cooled to room temperature to give a suspension, which was filtered. The cake was washed with water and dried under house vacuum for 18 h. The cake was then washed with ether and dried to give (53.84 g, 67%) of 1,1-dimethylethyl 5-(4-amino-7-methyl-7H-pyrrolo[2,3-*d*]pyrimidin-5-yl)-2,3-dihydro-1H-indole-1-carboxylate as a light gray solid. LC-MS (ES) *m/z* = 366.3 [M + H]⁺. ¹H NMR (400 MHz, DMSO-*d*₆) ppm 8.14 (s, 1 H), 7.76 (br s, 1 H), 7.26 (s, 1 H), 7.15–7.24 (m, 2 H), 6.05 (br s, 2 H), 3.95 (t, *J* = 8.7 Hz, 2 H), 3.73 (s, 3 H), 3.12 (t, *J* = 8.6 Hz, 2 H), 1.52 (br s, 9 H).

1,1-Dimethylethyl 5-(4-amino-7-methyl-7H-pyrrolo[2,3-*d*]pyrimidin-5-yl)-2,3-dihydro-1H-indole-1-carboxylate (3.10 g, 8.48 mmol) was dissolved in a mixture of 2 N HCl (17 mL) and EtOH (40 mL) as a dark solution. This mixture was filtered through Celite, washing with 50 mL of 4/1 EtOH/water. The filtrates were heated in an oil bath at 85 °C (gentle reflux) under nitrogen for 5 h. The clear brownish solution was cooled to room temperature and concentrated in vacuo. The slightly wet residue was diluted with 25 mL of EtOH and heated in a water bath at 65 °C for 5 min. The suspension was cooled to room temperature. The suspension was filtered, and the cake was washed with cold EtOH (6 mL) and EtOAc (6 mL). The solids were dried under vacuum at room temperature for 20 h to give 5-(2,3-dihydro-1H-indol-5-yl)-7-methyl-7H-pyrrolo[2,3-*d*]pyrimidin-4-amine-2HCl (2.37 g, 83%) as a light tan powder. LC-MS (ES) *m/z* = 266 [M + H]⁺. ¹H NMR (400 MHz, DMSO-*d*₆) 3.20 (t, *J* = 7.8 Hz, 2H), 3.70 (t, *J* = 8.0 Hz, 2H), 3.85 (s, 3H), 7.27–7.39 (m, 2H), 7.43 (s, 1 H), 7.65 (s, 1 H), 7.77–8.25 (br s, 1 H), 8.53 (s, 1 H).

To a solution of 5-(2,3-dihydro-1H-indol-5-yl)-7-methyl-7H-pyrrolo[2,3-*d*]pyrimidin-4-amine-2HCl (200 mg, 0.6 mmol), (2,5-difluorophenyl)acetic acid (120 mg, 0.696 mmol), and HATU (265 mg, 0.696 mmol) in DMF (5 mL) was added DIPEA (0.463 mL, 2.65 mmol). The mixture was stirred at room temperature overnight. LC-MS showed the reaction was completed. The mixture was poured into water. The precipitated solid was filtered and dried to afford 5-[1-[(2,5-difluorophenyl)acetyl]-2,3-dihydro-1H-indol-5-yl]-7-methyl-7H-pyrrolo[2,3-*d*]pyrimidin-4-amine (28) as a white solid (208 mg, 74%). ¹H NMR showed there is 1 equiv of DMF present. LC-MS (ES) *m/z* = 420 [M + H]⁺. ¹H NMR (400 MHz, DMSO-*d*₆) 3.27 (t, *J* = 8.46 Hz, 2 H), 3.74 (s, 3 H), 3.95 (s, 2 H), 4.29 (t, *J* = 8.46 Hz, 2 H), 6.05 (br s, 2 H), 7.21–7.27 (m, 5 H), 7.34 (s, 1 H), 8.09 (d, *J* = 8.34 Hz, 1 H), 8.15 (s, 1 H).

5-[1-[(2-Fluorophenyl)acetyl]-2,3-dihydro-1H-indol-5-yl]-7-methyl-7H-pyrrolo[2,3-*d*]pyrimidin-4-amine (29). To a solution of 5-(2,3-dihydro-1H-indol-5-yl)-7-methyl-7H-pyrrolo[2,3-*d*]pyrimidin-4-amine-2HCl (70.6 mg, 0.21 mmol), (2-fluorophenyl)acetic acid (32.2 mg, 0.209 mmol), and HATU (79 mg, 0.209 mmol)

in DMF (2 mL) was added DIPEA (0.15 mL, 0.84 mmol). The mixture was stirred at room temperature overnight. The mixture was poured into water, and the precipitated solid was collected and dried to afford 5-{1-[(2-fluorophenyl)acetyl]-2,3-dihydro-1H-indol-5-yl}-7-methyl-7H-pyrrolo[2,3-d]pyrimidin-4-amine (29) (73 mg, 84%). ¹H NMR (400 MHz, DMSO-*d*₆) 3.26 (t, *J* = 8.72 Hz, 2 H), 3.73 (s, 3 H), 3.93 (s, 2 H), 4.28 (t, *J* = 8.46 Hz, 2 H), 7.19 (d, *J* = 7.58 Hz, 3 H), 7.26 (s, 1 H), 7.30–7.38 (m, 3 H), 8.09 (d, *J* = 8.34 Hz, 1 H), 8.14 (s, 1 H). LC–MS (ES) *m/z* = 402.3 [M + H]⁺.

5-{1-[(3-Fluorophenyl)acetyl]-2,3-dihydro-1H-indol-5-yl}-7-methyl-7H-pyrrolo[2,3-d]pyrimidin-4-amine (30). To a solution of 5-(2,3-dihydro-1H-indol-5-yl)-7-methyl-7H-pyrrolo[2,3-d]pyrimidin-4-amine-2HCl (70.6 mg, 0.21 mmol), (3-fluorophenyl)acetic acid (32.2 mg, 0.209 mmol), and HATU (79 mg, 0.209 mmol) in DMF (2 mL) was added DIPEA (0.146 mL, 0.836 mmol). The mixture was stirred at room temperature overnight. The mixture was poured into water, and the precipitated solid was collected and dried to afford 5-{1-[(3-fluorophenyl)acetyl]-2,3-dihydro-1H-indol-5-yl}-7-methyl-7H-pyrrolo[2,3-d]pyrimidin-4-amine (30) as a white solid (81 mg, 96%). ¹H NMR (400 MHz, DMSO-*d*₆) 3.23 (t, *J* = 8.46 Hz, 2 H), 3.73 (s, 3 H), 3.92 (s, 2 H), 4.19–4.26 (m, 2 H), 7.08–7.11 (m, 1 H), 7.12–7.17 (m, 2 H), 7.23 (d, *J* = 8.34 Hz, 1 H), 7.25 (s, 1 H), 7.31 (s, 1 H), 7.36 (s, 1 H), 7.39 (d, *J* = 6.82 Hz, 1 H), 8.10–8.17 (m, 2 H). LC–MS (ES) *m/z* = 402.3 [M + H]⁺.

5-{1-[(4-Fluorophenyl)acetyl]-2,3-dihydro-1H-indol-5-yl}-7-methyl-7H-pyrrolo[2,3-d]pyrimidin-4-amine (31). To a solution of 5-(2,3-dihydro-1H-indol-5-yl)-7-methyl-7H-pyrrolo[2,3-d]pyrimidin-4-amine-2HCl (70 mg, 0.21 mmol), (4-fluorophenyl)acetic acid (37.5 mg, 0.244 mmol), and HATU (93 mg, 0.244 mmol) in DMF (2 mL) was added DIPEA (0.162 mL, 0.928 mmol). The mixture was stirred overnight. The mixture was poured into water (100 mL), and an off-white solid was formed. The solid was filtered, washed with water (10 mL), and dried to afford 81 mg (84%) of 5-{1-[(4-fluorophenyl)acetyl]-2,3-dihydro-1H-indol-5-yl}-7-methyl-7H-pyrrolo[2,3-d]pyrimidin-4-amine (31) as an off-white solid. LC–MS (ES) *m/z* = 402.3 [M + H]⁺. ¹H NMR (400 MHz, DMSO-*d*₆) 3.23 (t, *J* = 8.34 Hz, 2 H), 3.73 (s, 3 H), 3.88 (s, 2 H), 4.23 (t, *J* = 8.46 Hz, 2 H), 7.15–7.20 (m, 2 H), 7.21–7.26 (m, 2 H), 7.30–7.37 (m, 3 H), 8.13 (d, *J* = 8.34 Hz, 1 H), 8.15 (s, 1 H).

7-Methyl-5-{1-[(2-methylphenyl)acetyl]-2,3-dihydro-1H-indol-5-yl}-7H-pyrrolo[2,3-d]pyrimidin-4-amine (32). To a solution of 5-(2,3-dihydro-1H-indol-5-yl)-7-methyl-7H-pyrrolo[2,3-d]pyrimidin-4-amine-2HCl (70.6 mg, 0.21 mmol), (2-methylphenyl)acetic acid (31.4 mg, 0.209 mmol), and HATU (79 mg, 0.209 mmol) in DMF (2 mL) was added DIPEA (0.146 mL, 0.836 mmol). The mixture was stirred at room temperature overnight. The mixture was poured into water (100 mL), and a white solid formed. EtOAc (100 mL) was used to extract the product. The organic phase was separated, dried (MgSO₄), and evaporated to give a white solid. The solid was sonicated in water (10 mL), then filtered and dried to afford 7-methyl-5-{1-[(2-methylphenyl)acetyl]-2,3-dihydro-1H-indol-5-yl}-7H-pyrrolo[2,3-d]pyrimidin-4-amine (32) (48 mg, 55%) as a white solid. LC–MS (ES) *m/z* = 398.3 [M + H]⁺. ¹H NMR (400 MHz, DMSO-*d*₆) 8.02–8.24 (m, 2 H), 7.32 (s, 1 H), 7.25 (s, 1 H), 7.12–7.24 (m, 5 H), 6.07 (br s, 2 H), 4.26 (t, *J* = 8.5 Hz, 2 H), 3.87 (s, 2 H), 3.73 (s, 3 H), 3.24 (t, *J* = 8.5 Hz, 2 H), 2.24 (s, 3 H).

7-Methyl-5-{1-[(3-methylphenyl)acetyl]-2,3-dihydro-1H-indol-5-yl}-7H-pyrrolo[2,3-d]pyrimidin-4-amine (33). To a solution of 5-(2,3-dihydro-1H-indol-5-yl)-7-methyl-7H-pyrrolo[2,3-d]pyrimidin-4-amine-2HCl (70.6 mg, 0.21 mmol), (3-methylphenyl)acetic acid (31.4 mg, 0.209 mmol), and HATU (79 mg, 0.209 mmol) in DMF (2 mL) was added DIPEA (0.146 mL, 0.836 mmol). The mixture was stirred at room temperature overnight. The mixture was poured into water (100 mL), and a light brown solid formed. The solid was filtered and dried to afford 7-methyl-5-{1-[(3-methylphenyl)acetyl]-2,3-dihydro-1H-indol-5-yl}-7H-pyrrolo[2,3-d]pyrimidin-4-amine (33) (48 mg, 55%). LC–MS (ES) *m/z* = 398.3 [M + H]⁺. ¹H NMR (400 MHz, DMSO-*d*₆) 2.30 (s, 3 H), 3.16–3.23 (m, 2 H), 3.72 (s, 3 H), 3.82 (s, 2 H), 4.17–4.24 (m, 2 H), 7.06–7.14 (m, 3 H), 7.20–7.27 (m, 3 H), 7.30 (s, 1 H), 8.11–8.18 (m, 2 H).

1-Methyl-3-{1-[(4-methylphenyl)acetyl]-2,3-dihydro-1H-indol-5-yl}-1H-pyrazolo[3,4-d]pyrimidin-4-amine (34). To a solution of 3-(2,3-dihydro-1H-indol-5-yl)-1-methyl-1H-pyrazolo[3,4-d]pyrimidin-4-amine-2HCl (70 mg, 0.21 mmol), (4-methylphenyl)acetic acid (31.0 mg, 0.206 mmol), and HATU (78 mg, 0.206 mmol) in DMF (2 mL) was added DIPEA (0.144 mL, 0.825 mmol). The mixture was stirred overnight and then was poured into water. The precipitated white solid was filtered to give 75 mg (88%) of 1-methyl-3-{1-[(4-methylphenyl)acetyl]-2,3-dihydro-1H-indol-5-yl}-1H-pyrazolo[3,4-d]pyrimidin-4-amine (34) LC–MS (ES) *m/z* = 398.3 [M + H]⁺. ¹H NMR (400 MHz, DMSO-*d*₆) 2.29 (s, 3 H), 3.23 (t, *J* = 8.46 Hz, 2 H), 3.83 (s, 2 H), 3.93 (s, 3 H), 4.18–4.25 (m, 2 H), 7.14–7.21 (m, 4 H), 7.44 (dd, *J* = 8.34, 1.77 Hz, 1 H), 7.50 (s, 1 H), 8.20 (d, *J* = 8.34 Hz, 1 H), 8.25 (s, 1 H).

5-{1-[(2-Chlorophenyl)acetyl]-2,3-dihydro-1H-indol-5-yl}-7-methyl-7H-pyrrolo[2,3-d]pyrimidin-4-amine (35). To a solution of 5-(2,3-dihydro-1H-indol-5-yl)-7-methyl-7H-pyrrolo[2,3-d]pyrimidin-4-amine-2HCl (70.6 mg, 0.21 mmol), (2-chlorophenyl)acetic acid (39.9 mg, 0.234 mmol), and HATU (89 mg, 0.234 mmol) in DMF (2 mL) was added DIPEA (0.163 mL, 0.936 mmol). The mixture was stirred at room temperature overnight, and then the mixture was poured into water (100 mL), precipitating an off-white solid. The solid was filtered and dried to afford 94 mg (94%) of 5-{1-[(2-chlorophenyl)acetyl]-2,3-dihydro-1H-indol-5-yl}-7-methyl-7H-pyrrolo[2,3-d]pyrimidin-4-amine (35) as an off-white solid. NMR indicated 0.8 equiv of DMF was present. LC–MS (ES) *m/z* = 418.3 [M + H]⁺. ¹H NMR (400 MHz, DMSO-*d*₆) 3.39 (m, 2 H), 3.73 (s, 3 H), 4.00 (s, 2 H), 4.29 (m, 2 H), 7.25 (m, 2 H), 7.30–7.36 (m, 3 H), 7.40 (d, *J* = 4.55 Hz, 1 H), 7.46 (s, 1 H), 8.09 (s, 1 H), 8.14 (s, 1 H).

5-{1-[(3-Chlorophenyl)acetyl]-2,3-dihydro-1H-indol-5-yl}-7-methyl-7H-pyrrolo[2,3-d]pyrimidin-4-amine (36). To a solution of 5-(2,3-dihydro-1H-indol-5-yl)-7-methyl-7H-pyrrolo[2,3-d]pyrimidin-4-amine-2HCl (70.6 mg, 0.21 mmol), (3-chlorophenyl)acetic acid (39.9 mg, 0.234 mmol), and HATU (89 mg, 0.234 mmol) in DMF (2 mL) was added DIPEA (0.16 mL, 0.94 mmol). The mixture was stirred at room temperature overnight and then was poured into water (100 mL). EtOAc (100 mL) was used to extract the product. The organic phase was dried (MgSO₄), filtered, and evaporated to dryness to give a purple solid that contained some starting material. The solid was sonicated in water (10 mL), then filtered and dried to afford 5-{1-[(3-chlorophenyl)acetyl]-2,3-dihydro-1H-indol-5-yl}-7-methyl-7H-pyrrolo[2,3-d]pyrimidin-4-amine as a purple solid. LC–MS (ES) *m/z* = 418.3 [M + H]⁺. ¹H NMR (400 MHz, DMSO-*d*₆) 3.24 (t, *J* = 8.59 Hz, 2 H), 3.73 (s, 3 H), 3.92 (s, 2 H), 4.23 (t, *J* = 8.46 Hz, 2 H), 6.10 (s, 2 H), 7.23 (d, *J* = 8.34 Hz, 1 H), 7.26–7.29 (m, 2 H), 7.31–7.33 (m, 1 H), 7.34–7.39 (m, 3 H), 8.12 (d, *J* = 8.34 Hz, 1 H), 8.15 (s, 1 H).

7-Methyl-5-{1-[(3-(methoxyloxy)phenyl)acetyl]-2,3-dihydro-1H-indol-5-yl}-7H-pyrrolo[2,3-d]pyrimidin-4-amine (37). To a solution of 5-(2,3-dihydro-1H-indol-5-yl)-7-methyl-7H-pyrrolo[2,3-d]pyrimidin-4-amine-2HCl (70.6 mg, 0.21 mmol), [3-(methoxyloxy)phenyl]acetic acid (38.9 mg, 0.234 mmol), and HATU (89 mg, 0.234 mmol) in DMF (2 mL) was added DIPEA (0.16 mL, 0.94 mmol). The mixture was stirred at room temperature overnight and was then poured into water (100 mL), precipitating an off-white solid. The solid was filtered off and dried to afford 7-methyl-5-{1-[(3-(methoxyloxy)phenyl)acetyl]-2,3-dihydro-1H-indol-5-yl}-7H-pyrrolo[2,3-d]pyrimidin-4-amine as an off-white solid (91 mg, 90%). LC–MS (ES) *m/z* = 414.3 [M + H]⁺. ¹H NMR (400 MHz, DMSO-*d*₆) 3.21 (t, *J* = 8.46 Hz, 2 H), 3.73 (s, 3H), 3.75 (s, 3H), 3.84 (s, 2 H), 4.20 (t, *J* = 8.46 Hz, 2 H), 6.06 (br s, 2 H), 6.82–6.90 (m, 3 H), 7.21–7.26 (m, 3 H), 7.28–7.31 (m, 1 H), 8.11–8.19 (m, 1 H), 8.14 (s, 1 H).

7-Methyl-5-{1-[(3-(trifluoromethyl)phenyl)acetyl]-2,3-dihydro-1H-indol-5-yl}-7H-pyrrolo[2,3-d]pyrimidin-4-amine (38). To a stirred suspension of 5-(2,3-dihydro-1H-indol-5-yl)-7-methyl-7H-pyrrolo[2,3-d]pyrimidin-4-amine-2HCl (20.0 g, 59.1 mmol, 1 equiv) and HATU (24.73 g, 65.0 mmol, 1.1 equiv) in DMF (160 mL) chilled in an ice bath was added DIEA (33.0 mL, 189 mmol, 3.2 equiv) in one portion. The mixture turned into a clear light brown solution. To this mixture was added [3-(trifluoromethyl)phenyl]acetic acid

(12.07 g, 59.1 mmol, 1 equiv) portionwise (2 g per 15 min) over a 2 h period. The cooling bath was removed upon completion of the addition. The mixture was stirred at ambient temperature for another 2.5 h and then poured into 1 L of ice cold water to form a suspension, which was filtered. The cake was washed with water and dried under house vacuum for 1.5 h. The solid was dissolved in 500 mL of 10% MeOH in CH₂Cl₂, dried over Na₂SO₄, filtered, and concentrated in vacuo to give the crude product (39.5 g) as a brown foam. The crude product was dissolved in 100 mL of CHCl₃, split into 12 equal portions, and chromatographed on silica gel cartridges (Analox SF40-115g) using a gradient elution of 1% A to 60% A in CHCl₃ (A was a mixture of 3200/800/80 CHCl₃/MeOH/NH₄OH). Impure product fractions were combined and chromatographed using a gradient elution of 1% B in EtOAc to 75% B in EtOAc (B was a mixture of 20% MeOH in EtOAc). The combined purified product was taken up in CHCl₃ (23 mL) and MTBE (140 mL) as a slurry, which was filtered. The cake was washed with MTBE (2 × 100 mL) and hexane (3 × 75 mL). The solids were then dried under vacuum at 65 °C for 48 h to afford 7-methyl-5-(1-[[3-(trifluoromethyl)phenyl]acetyl]-2,3-dihydro-1H-indol-5-yl)-7H-pyrrolo[2,3-d]pyrimidin-4-amine (38) (20.64 g, 75%) as a white solid. LC-MS (ES) *m/z* = 452 [M + H]⁺. ¹H NMR (400 MHz, DMSO-*d*₆) 3.25 (t, *J* = 8.3 Hz, 2H), 3.73 (s, 1H), 4.03 (s, 2H), 4.27 (t, *J* = 8.5 Hz, 2H), 7.18–7.28 (m, 2H), 7.32 (s, 1H), 7.55–7.67 (m, 3H), 7.68 (s, 1H), 8.07–8.14 (m, 1H), 8.15 (s, 1H). Anal. Calcd for C₂₄H₂₀F₃N₅O: 63.85% C, 4.47% H, 15.69% N. Found: 63.82% C, 4.50% H, 15.70% N.

5-(1-[[3-Fluoro-5-(trifluoromethyl)phenyl]acetyl]-2,3-dihydro-1H-indol-5-yl)-7-methyl-7H-pyrrolo[2,3-d]pyrimidin-4-amine (39). A solution of 5-(2,3-dihydro-1H-indol-5-yl)-7-methyl-7H-pyrrolo[2,3-d]pyrimidin-4-amine 2HCl (150 mg, 0.443 mmol), [3-fluoro-5-(trifluoromethyl)phenyl]acetic acid (99 mg, 0.443 mmol), HATU (169 mg, 0.443 mmol), and DIEA (0.310 mL, 1.774 mmol) was stirred at room temperature overnight. The reaction mixture was poured into water (10 mL), and a precipitate formed. The precipitate was collected by filtration, and the residue was washed with water (10 mL) and dried. The beige solid was adsorbed onto silica and purified by flash chromatography (0–10% methanol in CH₂Cl₂, 12 g silica column) to afford a pale yellow solid which showed the presence of bis-acylated material. The product was adsorbed onto silica and purified by flash chromatography (100% EtOAc to 10% MeOH in EtOAc, then 10% MeOH in CH₂Cl₂, 12 g column) to afford 5-(1-[[3-fluoro-5-(trifluoromethyl)phenyl]acetyl]-2,3-dihydro-1H-indol-5-yl)-7-methyl-7H-pyrrolo[2,3-d]pyrimidin-4-amine (39) (110 mg, 53% yield) as a white solid. LC-MS (ES) *m/z* = 470 [M + H]⁺. ¹H NMR (400 MHz, DMSO-*d*₆) 3.27 (t, *J* = 8.34 Hz, 2H), 3.74 (s, 3H), 4.07 (s, 2H), 4.27 (t, *J* = 8.46 Hz, 2H), 5.81–6.32 (m, 2H), 7.17–7.29 (m, 2H), 7.33 (s, 1H), 7.52 (d, *J* = 9.60 Hz, 1H), 7.55–7.63 (m, 2H), 8.11 (d, *J* = 8.34 Hz, 1H), 8.15 (s, 1H).

7-Methyl-5-[1-[[2,3,5-trifluorophenyl]acetyl]-2,3-dihydro-1H-indol-5-yl]-7H-pyrrolo[2,3-d]pyrimidin-4-amine (40). A solution of 5-(2,3-dihydro-1H-indol-5-yl)-7-methyl-7H-pyrrolo[2,3-d]pyrimidin-4-amine (150 mg, 0.443 mmol), (2,3,5-trifluorophenyl)acetic acid (84 mg, 0.443 mmol), HATU (169 mg, 0.443 mmol), and DIEA (0.310 mL, 1.774 mmol) was stirred at room temperature overnight. The reaction mixture was poured into water (10 mL), and a precipitate formed. The precipitate was collected by filtration, washed with water (10 mL), and dried. The solid was adsorbed onto silica and purified by flash chromatography (0–10% methanol in DCM, 12-g column) to afford a pale yellow solid which showed the presence of bis-acylated material. The product was adsorbed onto silica and purified by flash chromatography (100% EtOAc to 10% MeOH in EtOAc, then 10% MeOH in CH₂Cl₂, 12 g column) to afford 7-methyl-5-[1-[[2,3,5-trifluorophenyl]acetyl]-2,3-dihydro-1H-indol-5-yl]-7H-pyrrolo[2,3-d]pyrimidin-4-amine (40) (102 mg, 53% yield) as a white solid. LC-MS (ES) *m/z* = 438 [M + H]⁺. ¹H NMR (DMSO-*d*₆, 400 MHz) 3.74 (s, 3H), 4.04 (s, 2H), 4.29 (t, *J* = 8.5 Hz, 2H), 6.08 (br s, 2H), 7.10–7.17 (m, 1H), 7.20–7.28 (m, 2H), 7.34 (s, 1H), 7.42–7.53 (m, 1H), 8.08 (d, *J* = 8.1 Hz, 1H), 8.15 (s, 1H). 3.28 (t, *J* = 8.3 Hz, 2H).

■ ASSOCIATED CONTENT

Supporting Information

Complete kinase profiling data for compound 38 and cloning, expression, purification, and crystallization details for human PERK with compounds 22 and 38. This material is available free of charge via the Internet at <http://pubs.acs.org>.

Accession Codes

Protein Data Bank submissions codes: compound 22, 4G34; compound 38, 4G31.

■ AUTHOR INFORMATION

Corresponding Author

*Telephone: 610-917-7899. E-mail: Jeffrey.M.Axten@gsk.com.

Notes

The authors declare no competing financial interest.

■ REFERENCES

- (1) Kim, I.; Xu, W.; Reed, J. C. Cell death and endoplasmic reticulum stress: disease relevance and therapeutic opportunities. *Nat. Rev. Drug Discovery* **2008**, *7*, 1013–1030.
- (2) Ma, Y.; Hendershot, L. M. The role of the unfolded protein response in tumour development: friend or foe? *Nat. Rev. Cancer* **2004**, *4*, 966–977.
- (3) Feldman, D. E.; Chauhan, V.; Koong, A. C. The unfolded protein response: a novel component of the hypoxic stress response in tumors. *Mol. Cancer Res.* **2005**, *3*, 597–605.
- (4) Koumenis, C.; Wouters, B. G. “Translating” tumor hypoxia: unfolded protein response (UPR)-dependent and UPR-independent pathways. *Mol. Cancer Res.* **2006**, *4*, 423–436.
- (5) Rouschop, K. M. A.; van den Beucken, T.; Dubois, L.; Niessen, H.; Bussink, J.; Savelkoul, K.; Keulers, T.; Mujcic, H.; Landuyt, W.; Voncken, J. W.; Lambin, P.; van der Kogel, A. J.; Koritzinsky, M.; Wouters, B. G. The unfolded protein response protects human tumor cells during hypoxia through regulation of the autophagy genes MAP1LC3B and ATG5. *J. Clin. Invest.* **2010**, *120*, 127–141.
- (6) Bi, M.; Naczki, C.; Koritzinsky, M.; Fels, D.; Blais, J.; Hu, N.; Harding, H.; Novoa, I.; Varia, M.; Raleigh, J.; Scheuner, D.; Kaufman, R. J.; Bell, J.; Ron, D.; Wouters, B. G.; Koumenis, C. ER stress-regulated translation increases tolerance to extreme hypoxia and promotes tumor growth. *EMBO J.* **2005**, *24*, 3470–3481.
- (7) Jorgensen, E.; Stinson, A.; Shan, L.; Yang, J.; Gietl, D.; Albino, A. P. Cigarette smoke induces endoplasmic reticulum stress and the unfolded protein response in normal and malignant human lung cells. *BMC Cancer* **2008**, *8*, 229–258.
- (8) Ameri, K.; Lewis, C. E.; Raida, M.; Sowter, H.; Hai, T.; Harris, A. L. Anoxic induction of ATF-4 through HIF-1-independent pathways of protein stabilization in human cancer cells. *Blood* **2004**, *103*, 1876–1882.
- (9) Davies, M. P.; Barraclough, D. L.; Stewart, C.; Joyce, K. A.; Eccles, R. M.; Barraclough, R.; Rudland, P. S.; Sibson, D. R. Expression and splicing of the unfolded protein response gene XBP-1 are significantly associated with clinical outcome of endocrine-treated breast cancer. *Int. J. Cancer* **2008**, *123*, 85–88.
- (10) Healy, S. J. M.; Gorman, A. M.; Mousavi-Shafaie, P.; Gupta, S.; Samali, A. Targeting the endoplasmic reticulum-stress response as an anticancer strategy. *Eur. J. Pharmacol.* **2009**, *625*, 234–246.
- (11) Ron, D.; Walter, P. Signal integration in the endoplasmic reticulum unfolded protein response. *Nat. Rev. Mol. Cell Biol.* **2007**, *8*, 519–529.
- (12) Koumenis, C.; Naczki, C.; Koritzinsky, M.; Rastani, S.; Diehl, A.; Sonenberg, N.; Koromilas, A.; Wouters, B. G. Regulation of protein synthesis by hypoxia via activation of the endoplasmic reticulum kinase PERK and phosphorylation of the translation initiation factor eIF2α. *Mol. Cell Biol.* **2002**, *22*, 7405–7416.
- (13) Blais, J. D.; Addison, C. L.; Edge, R.; Falls, T.; Zhao, H.; Wary, K.; Koumenis, C.; Harding, H. P.; Ron, D.; Holcik, M.; Bell, J. C.

PERK-dependent translation regulation promotes tumor cell adaptation and angiogenesis in response to hypoxic stress. *Mol. Cell. Biol.* **2006**, *26*, 9517–9532.

(14) Ghosh, R.; Lipson, K. L.; Sargent, K. E.; Mercurio, A. M.; Hunt, J. S.; Ron, D.; Urano, F. Transcriptional regulation of VEGF-A in the unfolded protein response pathway. *PLoS One* **2010**, *5*, e9575.

(15) Pereira, E. R.; Liao, N.; Neale, G. A.; Hendershot, L. M. Transcriptional and post-transcriptional regulation of proangiogenic factors by the unfolded protein response. *PLoS One* **2010**, *5*, e12521.

(16) Shi, Y.; Vattem, K. M.; Sood, R.; An, J.; Liang, J.; Stramm, L.; Wek, R. C. Identification and characterization of pancreatic eukaryotic initiation factor 2 alpha-subunit kinase, PEK, involved in translational control. *Mol. Cell. Biol.* **1998**, *18*, 7499–7509.

(17) Harding, H. P.; Zhang, Y.; Ron, D. Protein translation and folding are coupled by an endoplasmic-reticulum-resident kinase. *Nature* **1999**, *397*, 271–274.

(18) Sood, R.; Porter, A. C.; Ma, K.; Quilliam, L. A.; Wek, R. C. Pancreatic eukaryotic initiation factor-2alpha kinase (PEK) homologues in humans, *Drosophila melanogaster* and *Caenorhabditis elegans* that mediate translational control in response to endoplasmic reticulum stress. *Biochem. J.* **2000**, *346* (Part 2), 281–293.

(19) Ma, K.; Vattem, K. M.; Wek, R. C. Dimerization and release of molecular chaperone inhibition facilitate activation of eukaryotic initiation factor-2 kinase in response to endoplasmic reticulum stress. *J. Biol. Chem.* **2002**, *277*, 18728–18735.

(20) Su, Q.; Wang, S.; Gao, H. Q.; Kazemi, S.; Harding, H. P.; Ron, D.; Koromilas, A. E. Modulation of the eukaryotic initiation factor 2 alpha-subunit kinase PERK by tyrosine phosphorylation. *J. Biol. Chem.* **2008**, *283*, 469–475.

(21) Bertolotti, A.; Zhang, Y.; Hendershot, L. M.; Harding, H. P.; Ron, D. Dynamic interaction of BiP and ER stress transducers in the unfolded-protein response. *Nat. Cell Biol.* **2000**, *2*, 326–332.

(22) Marciniak, S. J.; Garcia-Bonilla, L.; Hu, J.; Harding, H. P.; Ron, D. Activation-dependent substrate recruitment by the eukaryotic translation initiation factor 2 kinase PERK. *J. Cell Biol.* **2006**, *172*, 201–209.

(23) See Supporting Information for PERK crystallography details. X-ray data were submitted to the Protein Data Bank (PDB code for compound **22** is 4G34, and that for **38** is 4G31).

(24) Abad-Zapatero, C.; Metz, J. T. Ligand efficiency indices as guideposts for drug discovery. *Drug Discovery Today* **2005**, *10*, 464–469.

(25) Liao, J. J. Molecular recognition of protein kinase binding pockets for design of potent and selective kinase inhibitors. *J. Med. Chem.* **2007**, *50*, 409–424.

(26) Cui, W.; Li, J.; Ron, D.; Sha, B. The structure of the PERK kinase domain suggests the mechanism for its activation. *Acta Crystallogr.* **2011**, *D67*, 423–428.

(27) Detailed biochemical characterization and structural data will be reported elsewhere.

(28) See Supporting Information for full profile and complete list of the kinases screened.

(29) All studies were conducted after review by the GSK Institutional Animal Care and Use Committee and in accordance with the GSK Policy on the Care, Welfare and Treatment of Laboratory Animals.

(30) Blais, J. D.; Addison, C. L.; Edge, R.; Falls, T.; Zhao, H.; Kishore, W.; Koumenis, C.; Harding, H. P.; Ron, D.; Holcik, M.; Bell, J. C. PERK-dependent translational regulation promotes tumor cell adaptation and angiogenesis in response to hypoxic stress. *Mol. Cell. Biol.* **2006**, *26*, 9517–9532.

(31) Miyazaki, Y.; Nakano, M.; Sato, H.; Truesdale, A. T.; Stuart, J. D.; Nartley, E. N.; Hightower, K. E.; Kane-Carson, L. Design and effective synthesis of novel templates, 3,7-diphenyl-4-amino-thieno and furo-[3,2-c]pyridines as protein kinase inhibitors and in vitro evaluation targeting angiogenic kinases. *Bioorg. Med. Chem. Lett.* **2007**, *17*, 250–254.

(32) Leonova, T. S.; Yashunskii, V. G. Some reactions of 4-aminopyrazolo[3,4-d]pyrimidines. *Chem. Heterocycl. Compd.* **1982**, *18*, 753–755.